

A combined multiscale finite element method based on the LOD technique for the multiscale elliptic problems with singularities

Kuokuo Zhang^{a,1}, Weibing Deng^{a,1,*}, Haijun Wu^{a,2}

^a*Department of Mathematics, Nanjing University, Nanjing 210093, People's Republic of China*

Abstract

In this paper, we construct a combined multiscale finite element method (MsFEM) using the Local Orthogonal Decomposition (LOD) technique to solve the multiscale problems which may have singularities in some special portions of the computational domain. For example, in the simulation of steady flow transporting through highly heterogeneous porous media driven by extraction wells, the singularities lie in the near-well regions. The basic idea of the combined method is to utilize the traditional finite element method (FEM) directly on a fine mesh of the problematic part of the domain and using the LOD-based MsFEM on a coarse mesh of the other part. The key point is how to define local correctors for the basis functions of the elements near the coarse and fine mesh interface, which require meticulous treatment. The proposed method takes advantages of the traditional FEM and the LOD-based MsFEM, which uses much less DOFs than the standard FEM and may be more accurate than the LOD-based MsFEM for problems with singularities. The error analysis is carried out for highly varying coefficients, without any assumptions on scale separation or periodicity. Numerical examples with periodic and random highly oscillat-

*Corresponding author

Email addresses: dg1721016@smail.nju.edu.cn (Kuokuo Zhang), wbdeng@nju.edu.cn (Weibing Deng), hjw@nju.edu.cn (Haijun Wu)

¹The work of this author was partially supported by the NSF of China grant 12090023 and 12171237, and by the Ministry of Science and Technology of China grant 2020YFA0713800.

²The work of this author was partially supported by the NSF of China grants 11071116, 91130004.

ing coefficients, as well as the multiscale problems on the L-shaped domain, and multiscale problems with high-contrast channels or well-singularities are presented to demonstrate the efficiency and accuracy of the proposed method.

Keywords: Multiscale problems, non-periodic, LOD, well-singularity, high-contrast channel.

2021 MSC: 34E13, 65N12, 65N30

1. Introduction

In this paper we consider the elliptic problems with rapidly varying (non-periodic) coefficients, which involve many spatial scales. Such problems are typically referred to as multiscale problems and often arisen in composite materials and flows in porous media. Any meaningful numerical simulation of these problems such as standard finite element method (FEM) has to account for the highly heterogeneous fine-scale structures in the whole computational domain. This means that the underlying computational mesh has to be sufficiently fine and hence requires an enormous computational demand.

In order to overcome this difficulty, many kinds of methods have been developed in recent decades to solve such multiscale problems. Roughly speaking, from the perspective of final approximation solution, these numerical methods can be categorized into two classes. One is to solve the original problem in the constructed coarse-grid multiscale basis function space hence obtains a good approximation of the original-problem solution; the other is to solve a macro model equivalent to the original problem on the coarse grid mesh hence grasps the macro behavior of the multiscale solution. See, for example, the generalized FEM (GFEM) [1, 2, 3], the multiscale FEM (MsFEM) [4, 5, 6], the variational multiscale methods (VMM) or residual-free bubbles method (RFBM) [7, 8, 9, 10], the heterogeneous multiscale methods (HMM) [11, 12, 13], the multiscale finite-volume method [14], the multigrid numerical homogenization techniques [15, 16], the mortar multiscale methods [17, 18], the localized orthogonal decomposition methods (LODM) [19, 20, 21], the equation-free ap-

proaches [22, 23], the generalized MsFEM (GMsFEM) [24, 25], the multiscale-
25 spectral GFEM (MS-GEFM) [26, 27], the constraint energy minimizing GMS-
FEM (CEM-GMsFEM)[28, 29, 30], some numerical homogenization methods or
upscaling methods [31, 32, 33, 34, 35], and so on.

Most of the above mentioned multiscale methods consist of two parts, one is
the macro solver on coarse mesh such as various finite element or finite volume
30 methods, and the other is the cell problems solving on the coarse grid or over-
sampling elements. The multiscale algorithm captures the fine-scale information
of the solution by solving the cell problems, and then uses the solutions of the
cell problems to form an equivalent macro model or a low dimensional multi-
scale approximation space of the solution. The definition of the cell problem
35 is mainly based on the differential operator of the original multiscale problem,
such as the elliptic operator, so that the variability of the multiscale coefficients
can be brought into the final solution model through the solution of the cell
problems.

In this paper, we are concerned with a special kind of multiscale problems
40 – those with singularities. For example, the one in L-region has singularity
near the corner; while the problem with high-contrast channel that connects
the boundaries of coarse-grid blocks has singularity at the edge of the channel
[36, 37, 38, 32]; furthermore, the problem with steady flow transporting through
highly heterogeneous porous media driven by extraction wells has singularity
45 near the well [39]. The traditional multiscale methods on coarse grids may be
inefficient when dealing with singularity. This is mainly because the local sin-
gularity of the solution is hard to be grasped effectively at the coarse grid level.
To solve this kind of singular problems, some numerical methods have been pro-
posed in the literature. See, for instance, the adaptive GMsFEM used to solve
50 the high contrast problem [40, 41], the MsFEM used to solve the high contrast
interface and channel problems [42, 36], the complete multiscale coarse grid algo-
rithm by using the Green functions for solving steady flow problem involving well
singularities in heterogeneous porous medium [39], the CEM-GMsFEM used to
solve the high contrast problem [28, 29], the LODM used to solve high contrast

55 and complex geometric boundary problems [21, 43, 44], the combined MsFEM
used to solve high contrast channel and well-singularity problems [45, 46], and
some generalized finite element methods and numerical homogenization meth-
ods used to solve high contrast problems [16, 26, 27, 31, 32], and so on. Among
them, most of the multiscale methods capture the small scale information of the
60 original-problem solution through the solution of the cell problems. Moreover,
for the problems with singularities, such as the problem with high-contrast and
narrow channels, in order to grasp the singularities, it needs to construct multi-
scale finite element approximation space via solving special cell problems. For
example, the CEM-GMsFEM first needs to construct the auxiliary multiscale
65 functions by solving the local spectral problem. Consequently, the auxiliary
function space is constructed by selecting the eigenfunctions corresponding to
small eigenvalues, which correspond to high contrast channels. Finally, the
online multiscale basis functions are constructed based on constrained energy
minimization in the auxiliary function space.

70 However, it is difficult to define the corresponding subproblems to construct
the required approximation space for the problems with source term singular-
ity, such as the porous medium flow problem with well singularities. In [45, 46],
the authors combined the standard FEM with the oversampling MsFEM and
Petrov-Galerkin MsFEM to solve the multiscale problem with singularity. The
75 standard FEM is used on a fine mesh of the problematic part of the domain and
the oversampling MsFEM or Petrov-Galerkin MsFEM is used on a coarse mesh
of the other part. The transmission condition on the interface between coarse
and fine meshes is dealt with the penalty technique. The proposed methods take
the advantages of the standard FEM and the MsFEM, and maintain the accu-
80 racy of the two methods. It is shown [45, 46] that the combined multiscale meth-
ods can solve the multiscale elliptic problems with fine and long-ranged high
contrast channels and the well singularities very efficiently. But, the error anal-
ysis of the methods is still based on the classical homogenization theory, which
requires the assumption that the diffusion coefficient is periodic. Therefore, how
85 to improve the algorithm so that the optimal error estimate can be obtained for

any diffusion coefficient needs further study. We remark that in the past decade, there are many nice multiscale methods dealing with arbitrary oscillating coefficients, such as the LODM, CEM-GMsFEM, MS-GFEM, and some numerical homogenization methods mentioned above [16, 19, 20, 21, 26, 27, 28, 29, 30, 31, 32].

90 In this paper, we focus on the LODM which was originally introduced in [19] and could be derived from the VMM framework [20, 21]. The orthogonal decomposition method starts from two finite element spaces, a coarse space V_H and a very high dimensional space V_h which can approximate the multiscale solution well. Further, the decomposition can be described in three steps: (1) define a
95 quasi-interpolation operator $I_H : V_h \rightarrow V_H$, (2) define a high dimensional space of negligible information by the kernel of the operator I_H , i.e. $W_h := \text{kern}(I_H)$, and (3) find the orthogonal complement of W_h in V_h with respect to the energy scalar product. With this strategy, it is possible to split the space V_h into the orthogonal direct sum of a low dimensional multiscale space V_H^{ms} and a high
100 dimensional remainder space W_h . The multiscale problem is solved in the low dimensional space V_H^{ms} and is therefore cheap. However, the construction of the exact splitting of $V_h = V_H^{ms} \oplus W_h$ is unpractical since it needs to define the correction operator in the whole domain which is computationally expensive. We call the method as an ideal one whose solution is referred as ideal solution. To
105 reduce the computational complexity, several localization strategies were proposed and analyzed in [19, 20, 21]. In fact, the computation of the orthogonal decomposition is localized to the patches of the elements, which we introduced as LODM. The reason which makes localization successful is that outside of the support of the coarse finite element basis functions of V_H , the canonical
110 basis functions of the multiscale space V_H^{ms} have the property of exponential decay. We remark that the LODM often use the fine-scale solution in V_h for comparison, which is referred to as reference solution.

The essence of the LODM is to construct a low-dimensional solution space (with a locally supported basis functions) that has very accurate approximation
115 properties with respect to the exact solution. So far, the idea of LOD has been generalized to several kinds of discretization techniques such as discontinuous

Galerkin [47], Petrov-Galerkin formulations [48] and mesh-free methods [49]. Moreover, the method has been successfully applied to many kinds of problems such as semi-linear elliptic problems [50], eigenvalue problems [51, 52], problems
120 on complicated geometries [43], and so on. We refer the reader to [53, 54] and references therein for more works about LODM. The attractive point of this method is that it does not rely on the classical homogenization theory and does not need the scale separation assumption.

Based on the above observation, we will use the LOD technique to improve
125 the combined MsFEM and make it suitable for general multiscale problems. Note that the traditional FEM has many excellences to deal with the singularities, such as, refining the mesh or enlarging the polynomial order of the finite element space. Thus, in order to take advantages of both methods, we introduce a combined FE and LOD method (FE-LODM) to solve the multiscale problems
130 with singularities. The idea of this approach is to utilize the traditional FEM directly on a fine mesh of the problematic part of the domain and use the LODM on a coarse mesh of the other part. Comparing to the implement of LODM, there are two key issues of the FE-LODM to consider. The first one is how to define the corresponding quasi-interpolation operator in the subdomain using
135 fine mesh. Here we just choose the L^2 projection Π_h , which has the property that $\Pi_h u_h = u_h$ for u_h belongs to the fine mesh linear FEM space. This property is very important in our later error analysis, which yields a very useful result that the ideal solution is equals to the reference solution in the subdomain using fine mesh. The second one is how to define the correction operators near the
140 interface between the coarse and fine mesh. A delicate treatment should be done for the elements who have an edge or face in the interface of coarse-fine mesh. For the introduced FE-LODM, we carry out a rigorous and careful analysis for the elliptic equation with arbitrary diffusion coefficient to show both the energy and L^2 errors of the method have the optimal convergence rate. The numerical
145 results also show that the proposed FE-LODM is very efficient for multiscale problems with random generated coefficients and singularities.

The rest of this paper is organized as follows. In Section 2, we give the

model problem and define a fine-scale reference problem. Section 3 is devoted to deriving the FE-LODM. In Section 4, we present the error analysis of the approach. In Section 5, we provide some numerical results to demonstrate the efficiency of our method. Conclusions are draw in the last section.

Throughout this paper, standard notations for Lebesgue and Sobolev spaces are employed, and C denotes the generic constant, which depends on neither the mesh size nor the diffusion coefficient. We also use the shorthand notation $a \lesssim b$ and $b \gtrsim a$ for the inequality $a \leq Cb$ and $b \geq Ca$. In addition, the shorthand notation $a \approx b$ represents that $a \lesssim b$ and $b \lesssim a$.

2. Model problem and reference approximations

In this section, we first present the multiscale model problem, then introduce its interior penalty continuous-discontinuous Galerkin (IPCDG) discretization on fine meshes and discuss the approximation errors of the IPCDG method. The IPCDG solution will be used as a fine-scale reference solution to estimate the error of the FE-LODM. Note that the IPCDG method was first introduced in [55] for the Helmholtz equation.

2.1. Model Problem

In this paper, we consider a second order elliptic problem with highly varying diffusion coefficient. Let $\Omega \subset \mathbb{R}^d$, $d=2,3$, be a polygonal/polyhedral domain, and the elliptic equation reads as

$$\begin{cases} -\nabla \cdot (A\nabla u) = f & \text{in } \Omega, \\ u = 0 & \text{on } \partial\Omega, \end{cases} \quad (2.1)$$

where we assume that $f \in L^2(\Omega)$, and the diffusion matrix $A \in L^\infty(\Omega, \mathbb{R}^{d \times d})$ is a symmetric matrix with uniform spectral bounds $\beta \geq \alpha > 0$, i.e.

$$\sigma(A(x)) \subset [\alpha, \beta] \quad \forall x \in \Omega. \quad (2.2)$$

The weak formulation of problem (2.1) is to find $u \in H_0^1(\Omega)$ such that

$$\int_{\Omega} A\nabla u \cdot \nabla v \, dx = \int_{\Omega} f v \, dx \quad \forall v \in H_0^1(\Omega). \quad (2.3)$$

165 Clearly, the Lax-Milgram lemma [56] implies that (2.3) has a unique solution.

In order to deal with the multiscale problem that has singularities, we decompose the research domain Ω into two parts, Ω_1 and Ω_2 , where Ω_1 consists of some subdomain(s) containing the singularities and $\Omega_2 = \Omega \setminus \overline{\Omega}_1$ (see Figure 1 for an illustration). Let $\Gamma = \partial\Omega_1 \cap \partial\Omega_2$ be the interface between Ω_1 and Ω_2 .
 170 We assume that the length/area of Γ satisfies $|\Gamma| = O(1)$, and Γ is Lipschitz continuous.

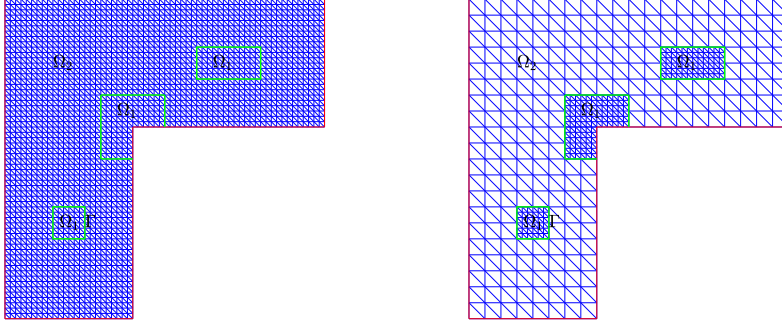


Figure 1: A decomposition of Ω into Ω_1 with singularities and $\Omega_2 = \Omega \setminus \overline{\Omega}_1$, where the green lines represent the interface Γ . Left: A fine-scale mesh for the reference problem; Right: A mesh for the combined multiscale methods.

For any subdomain $\omega \subseteq \Omega$, we denote by $(u, v)_\omega = \int_\omega uv$. For any segment/patch $\gamma \subseteq \Gamma$, denote by $\langle u, v \rangle_\gamma = \int_\gamma uv$. For brevity, let $(u, v) = (u, v)_\Omega$, $(\nabla u, \nabla v) = (\nabla u, \nabla v)_\Omega$ and $\langle u, v \rangle = \langle u, v \rangle_\Gamma$.

175 2.2. Reference problem

In this subsection, we introduce the IPCDG method which will be used as the fine-scale reference problem to estimate the error of our FE-LODM.

Let \mathcal{M}_{h,Ω_1} and \mathcal{M}_{h,Ω_2} be regular and quasi-uniform triangulations of Ω_1 and Ω_2 , respectively. Denote by $\mathcal{M}_{h,h} := \mathcal{M}_{h,\Omega_1} \cup \mathcal{M}_{h,\Omega_2}$ the resulted triangulation
 180 of Ω . Note that any element in the triangulation is considered closed by convention. For any $T \in \mathcal{M}_{h,h}$, let $h_T := \text{diam } T$. Denote by $h := \max_{T \in \mathcal{M}_{h,h}} h_T$.

Let \mathbf{n} be the unit normal vector of Γ that points from Ω_1 to Ω_2 . We define the jump and average of a function v across Γ by $[v] := v|_{\Omega_1} - v|_{\Omega_2}$ and $\{v\} := (v|_{\Omega_1} + v|_{\Omega_2})/2$, respectively. Moreover, we denote by ∇_h the piecewise
185 gradient on $\Omega_1 \cup \Omega_2$, that is, $\nabla_h v|_{\Omega_i} = \nabla(v|_{\Omega_i}), i = 1, 2$.

Denote by $\Gamma_i = \partial\Omega \cap \partial\Omega_i$ and

$$H_{\Gamma_i}^1(\Omega_i) := \{v \in H^1(\Omega_i) : v|_{\Gamma_i} = 0 \text{ in the sense of trace}\}, i = 1, 2.$$

Let V_{h,Ω_i} be the continuous linear Lagrange finite element space on $\mathcal{M}_{h,\Omega_i}, i = 1, 2$, respectively, i.e.

$$V_{h,\Omega_i} := \{v_h \in H_{\Gamma_i}^1(\Omega_i) : v_h|_T \in P_1, \forall T \in \mathcal{M}_{h,\Omega_i}\},$$

where P_1 is the set of polynomials with total degree ≤ 1 . Then the approximation space of the fine-scale reference problem is defined by

$$V_{h,h} := \{v_h : v_h|_{\Omega_i} \in V_{h,\Omega_i}, i = 1, 2\}. \quad (2.4)$$

Note that a discrete function in $V_{h,h}$ is continuous on each $\Omega_i, i = 1, 2$, but may be discontinuous across the interface Γ . Given some positive penalty parameters $\gamma_0 > 0$, for any subset $\omega \subseteq \Omega$, we define a symmetric bilinear form $a_\omega(\cdot, \cdot)$ as follows:

$$a_\omega(u, v) := (A\nabla_h u, \nabla_h v)_\omega - (\langle \{A\nabla_h u \cdot \mathbf{n}\}, [v] \rangle_{\Gamma \cap \omega} + \langle [u], \{A\nabla_h v \cdot \mathbf{n}\} \rangle_{\Gamma \cap \omega}) + J_\omega(u, v), \quad (2.5)$$

$$J_\omega(u, v) := \left\langle \frac{\gamma_0}{h} [u], [v] \right\rangle_{\Gamma \cap \omega}. \quad (2.6)$$

Then the IPCDG method (cf. [55]) reads as: find $u_{h,h} \in V_{h,h}$, such that

$$a_\Omega(u_{h,h}, v_{h,h}) = (f, v_{h,h}) \quad \forall v_{h,h} \in V_{h,h}. \quad (2.7)$$

Remark 1. (1) Noticed that $u_{h,h}$ is continuous in Ω_2 and subdomain(s) in Ω_1 and that the discontinuities across the interface Γ is treated by the interior penalty technique from the IPDG methods [57], so we call this method (2.7) the IPCDG method.

(2) It is easy to verify that the IPCDG method is consistent with the multi-scale problem (2.1), that is

$$a_\Omega(u - u_{h,h}, v_{h,h}) = 0 \quad \forall v_{h,h} \in V_{h,h}.$$

Introduce the discrete energy norm

$$\|v\|_{h,h} = \left(\|A^{\frac{1}{2}} \nabla_h v\|_{0,\Omega}^2 + \frac{\gamma_0}{h} \|v\|_\Gamma^2 + \frac{h}{\gamma_0} \|\{A \nabla_h v \cdot \mathbf{n}\}\|_\Gamma^2 \right)^{\frac{1}{2}}.$$

Clearly, the bilinear form a_Ω is continuous on $V \times V$ where $V := \{v : v|_{\Omega_i} \in H^2(\Omega_i) \cap H_{\Gamma_i}^1(\Omega_i), i = 1, 2\}$, i.e.

$$|a_\Omega(u, v)| \lesssim \|u\|_{h,h} \|v\|_{h,h}. \quad (2.8)$$

Following [55, 57], it may be proved that there exists a positive constant α_0 such that

$$a_\Omega(v_{h,h}, v_{h,h}) \gtrsim \|v_{h,h}\|_{h,h}^2 \quad v_{h,h} \in V_{h,h}, \quad \text{if } \gamma_0 \geq \alpha_0, \quad (2.9)$$

190 and hence the following Céa's lemma and the well-posedness hold for the IPCDG method (2.7) if the penalty parameter $\gamma_0 \geq \alpha_0$. We omitted the details.

Lemma 2.1. *Suppose $\gamma_0 \geq \alpha_0$. Then the following error estimate holds:*

$$\|u - u_{h,h}\|_{h,h} \lesssim \inf_{v_{h,h} \in V_{h,h}} \|u - v_{h,h}\|_{h,h}.$$

Then the error estimate of the IPCDG method may be obtained by combining the above Céa's lemma and the interpolation error estimates. We omitted the details and just assume that the IPCDG solution $u_{h,h}$ is a good approxima-
 195 tion of the exact solution u . We will use $u_{h,h}$ as a reference solution to estimate the error of our FE-LODM.

For further error analysis, we introduce the following norm on the restriction of the space $V_{h,h}$ onto a subdomain $\omega \subseteq \Omega$:

$$\|v\|_{h,h,\omega} = \left(\|A^{\frac{1}{2}} \nabla_h v\|_{0,\omega}^2 + \frac{\gamma_0}{h} \|v\|_{\Gamma \cap \omega}^2 \right)^{\frac{1}{2}} \quad (2.10)$$

and denote by $\|\cdot\|_{h,h} := \|\cdot\|_{h,h,\Omega}$ the norm on the whole domain Ω . Noting that the norm $\|\cdot\|_{h,h}$ is just the norm $\|\cdot\|_{h,h}$ with the third term dropped, by using the trace and inverse inequalities [56], it is easy to show that the two norms are
 200 equivalent on the fine-scale approximation space $V_{h,h}$.

3. FE-LODM formulation

In this section, we will present the FE-LODM which uses FEM in the domain Ω_1 containing singularities and LODM in Ω_2 where the solution is smooth but highly oscillating and the two methods are joint at the interface Γ by using the interior penalty technique. To do this, we first introduce coarse meshes on Ω_2 and coarse-scale finite element spaces, secondly state the multiscale decomposition of the fine-scale space $V_{h,h}$ and the approximation space for the FE-LODM, then present the ideal combined multiscale method, and finally formulate the localized combined multiscale method, i.e., FE-LODM.

3.1. Coarse-scale FE spaces

Let \mathcal{M}_{H,Ω_2} a shape-regular coarse triangulation of Ω_2 such that the fine reference mesh \mathcal{M}_{h,Ω_2} is a refinement of it. Denote by H the maximum diameter of elements in \mathcal{M}_{H,Ω_2} . Clearly, $h < H$. Let \mathcal{M}_{Γ_h} and \mathcal{M}_{Γ_H} be the set of interface elements in \mathcal{M}_{h,Ω_1} and \mathcal{M}_{H,Ω_2} , respectively, i.e.

$$\mathcal{M}_{\Gamma_h} := \{T \in \mathcal{M}_{h,\Omega_1} : |T \cap \Gamma| \neq 0\} \text{ and } \mathcal{M}_{\Gamma_H} := \{T \in \mathcal{M}_{H,\Omega_2} : |T \cap \Gamma| \neq 0\}.$$

Denote by $\Gamma_h := \{T \cap \Gamma : T \in \mathcal{M}_{\Gamma_h}\}$ and $\Gamma_H := \{T \cap \Gamma : T \in \mathcal{M}_{\Gamma_H}\}$ the two partitions of the interface Γ induced by \mathcal{M}_{h,Ω_1} and \mathcal{M}_{H,Ω_2} , respectively. In addition, we assume that \mathcal{M}_{h,Ω_1} and \mathcal{M}_{H,Ω_2} satisfy the matching condition that Γ_h is a refinement of Γ_H . Introduce the coarse-scale finite element space on the coarse mesh \mathcal{M}_{H,Ω_2} :

$$V_{H,\Omega_2} := \{v_H \in H_{\Gamma_2}^1(\Omega_2) : v_H|_T \in P_1, \forall T \in \mathcal{M}_{H,\Omega_2}\}.$$

Let

$$V_{h,H} := \{v_{h,H} : v_{h,H}|_{\Omega_1} \in V_{h,\Omega_1}, v_{h,H}|_{\Omega_2} \in V_{H,\Omega_2}\}.$$

Moreover, we denote by

$$V_{0,h} := \{v_{h,h} \in V_{h,h} : v_{h,h}|_{\Omega_1} = 0\} \text{ and } V_{0,H} := \{v_{h,H} \in V_{h,H} : v_{h,H}|_{\Omega_1} = 0\}.$$

3.2. Multiscale Decomposition

First, we need to define a quasi-interpolation operator from the fine-scale approximation space to the coarse-scale space. For this, we first introduce a weighted Clément-type quasi-interpolation operator \mathcal{C}_H defined on the region Ω_2 (see [58, 59]). Let \mathcal{N}_H be the set of vertices of elements in \mathcal{M}_{H,Ω_2} and let $\mathring{\mathcal{N}}_H := \mathcal{N}_H \setminus \Gamma_2$. For any node $z \in \mathring{\mathcal{N}}_H$, let $\Phi_z \in V_{H,\Omega_2}$ be the nodal basis function at z . The Clément-type quasi-interpolation operator $\mathcal{C}_H: H_{\Gamma_2}^1(\Omega_2) \mapsto V_{H,\Omega_2}$ is given by:

$$\mathcal{C}_H u := \sum_{z \in \mathring{\mathcal{N}}_H} u_z \Phi_z \quad \text{with } u_z = \frac{(u, \Phi_z)_{\Omega_2}}{(1, \Phi_z)_{\Omega_2}} \quad \forall u \in H_{\Gamma_2}^1(\Omega_2). \quad (3.1)$$

Further, let $\Pi_h: L^2(\Omega_1) \mapsto V_{h,\Omega_1}$ be the L^2 -projection operator. Clearly,

$$\Pi_h v_h = v_h \quad \forall v_h \in V_{h,\Omega_1}. \quad (3.2)$$

Then the quasi-interpolation operator $\mathcal{C}_{h,H}: V_{h,h} \mapsto V_{h,H}$ can be defined as

$$\begin{cases} \mathcal{C}_{h,H} v_{h,h}|_{\Omega_1} := \Pi_h(v_{h,h}|_{\Omega_1}); \\ \mathcal{C}_{h,H} v_{h,h}|_{\Omega_2} := \mathcal{C}_H(v_{h,h}|_{\Omega_2}), \end{cases} \quad \text{for any } v_{h,h} \in V_{h,h}. \quad (3.3)$$

By the operator $\mathcal{C}_{h,H}$, we can define its kernel space $W_{h,h} := \{v_{h,h} \in V_{h,h} \mid \mathcal{C}_{h,H} v_{h,h} = 0\}$, and use it to construct a splitting of the space $V_{h,h}$ into the direct sum

$$V_{h,h} = V_{h,H} \oplus W_{h,h}. \quad (3.4)$$

Notice that, for any $w_{h,h} \in W_{h,h}$, from (3.2) it follows that $w_{h,h}|_{\Omega_1} = 0$. Hence, in the following, we change the notation $W_{h,h}$ into $W_{0,h}$ for emphasis.

215 Note that the subspace $W_{0,h}$ is a fine-scale remainder space (high-dimensional space), which contains the fine-scale features of $V_{0,h}$ that can not be expressed in the low-dimensional space $V_{0,H}$. Following the idea of LODM ([21, 50]), we look for a splitting $V_{h,h} = V_{h,H}^{ms} \oplus W_{0,h}$ such that the space $V_{h,H}^{ms}$ has good H^1 approximation properties to the solution of the multiscale problem. It is obvious that $V_{h,H}^{ms}$ is a low-dimensional space that it has the same dimension as

220

$V_{h,H}$. In order to explicitly construct such a splitting, we look for the orthogonal complement of $W_{0,h}$ in $V_{h,h}$ with respect to the scalar product $a_\Omega(\cdot, \cdot)$.

The corresponding fine-scale projection $Q_h: V_{h,h} \mapsto W_{0,h}$ is given by: for $v_{h,h} \in V_{h,h}$, find $Q_h v_{h,h} \in W_{0,h}$, such that

$$a_\Omega(Q_h v_{h,h}, w_{0,h}) = a_\Omega(v_{h,h}, w_{0,h}) \quad \forall w_{0,h} \in W_{0,h}. \quad (3.5)$$

Using the fine-scale projection, we can define the approximation space on the whole domain Ω for the ideal combined multiscale method by

$$V_{h,H}^{ms} := (I - Q_h)V_{h,H}. \quad (3.6)$$

3.3. The ideal combined multiscale method

Next, we define the ideal combined multiscale method for the problem (2.7) as follows: for all $v_{h,H}^{ms} \in V_{h,H}^{ms}$, find $u_{h,H}^{ms} \in V_{h,H}^{ms}$, such that

$$a_\Omega(u_{h,H}^{ms}, v_{h,H}^{ms}) = (f, v_{h,H}^{ms}). \quad (3.7)$$

With above definition of the ideal method, we can see that, by taking $v_{h,H}^{ms} = u_{h,H}^{ms}$ in (3.7) and using the coercivity (2.9) of a_Ω on $V_{h,h}$, we have the following stability for the ideal solution $u_{h,H}^{ms}$: if $\gamma_0 \geq \alpha_0$,

$$\|u_{h,H}^{ms}\|_{h,h} \lesssim \|f\|_{L^2(\Omega)}. \quad (3.8)$$

Remark 2. *It can be proved that $\mathcal{C}_{h,H}$ is an isomorphism on $V_{h,H}$ (see Lemma 4.4).*

Thus we can split $u_{h,H}^{ms}$ into

$$u_{h,H}^{ms} = \underbrace{(\mathcal{C}_{h,H}|_{V_{h,H}})^{-1} \mathcal{C}_{h,H} u_{h,H}^{ms}}_{\in V_{h,H}} - \underbrace{((\mathcal{C}_{h,H}|_{V_{h,H}})^{-1} \mathcal{C}_{h,H} u_{h,H}^{ms} - u_{h,H}^{ms})}_{\in W_{0,h}}.$$

Moreover, it is easy to check that

$$(\mathcal{C}_{h,H}|_{V_{h,H}})^{-1} \mathcal{C}_{h,H} u_{h,H}^{ms} - u_{h,H}^{ms} = Q_h((\mathcal{C}_{h,H}|_{V_{h,H}})^{-1} \mathcal{C}_{h,H} u_{h,H}^{ms}).$$

Therefore, we have the splitting that obeys (3.6)

$$u_{h,H}^{ms} = u_{h,H} - Q_h(u_{h,H}), \quad \text{where } u_{h,H} := (\mathcal{C}_{h,H}|_{V_{h,H}})^{-1} \mathcal{C}_{h,H} u_{h,H}^{ms}. \quad (3.9)$$

It is clear that $\mathcal{C}_{h,H} u_{h,H}^{ms} = \mathcal{C}_{h,H} u_{h,H}$.

Before closing this subsection, we present an interesting result in the following proposition about the ideal method (3.7) which says that there is no difference between the ideal solution and the reference solution in the subdomain Ω_1 .

Proposition 1. *Let $u_{h,h}$ and $u_{h,H}^{ms}$ be the solutions to (2.7) and (3.7), respectively. Then we have*

$$u_{h,h} - u_{h,H}^{ms} \in W_{0,h} \quad \text{and} \quad \mathcal{C}_{h,H}u_{h,h} = \mathcal{C}_{h,H}u_{h,H}, \quad (3.10)$$

where $u_{h,H}$ is defined in Remark 2. Especially, $u_{h,h}|_{\Omega_1} = u_{h,H}^{ms}|_{\Omega_1}$.

Proof. Form (2.7) and (3.7), for all $v_{h,H}^{ms} \in V_{h,H}^{ms}$, it follows that

$$\begin{aligned} a_{\Omega}(u_{h,h}, v_{h,H}^{ms}) &= (f, v_{h,H}^{ms}), \\ a_{\Omega}(u_{h,H}^{ms}, v_{h,H}^{ms}) &= (f, v_{h,H}^{ms}). \end{aligned}$$

Thus

$$a_{\Omega}(u_{h,h} - u_{h,H}^{ms}, v_{h,H}^{ms}) = 0, \quad (3.11)$$

which means $u_{h,h} - u_{h,H}^{ms} \in W_{0,h}$. Hence

$$\mathcal{C}_{h,H}u_{h,h} = \mathcal{C}_{h,H}u_{h,H}^{ms} = \mathcal{C}_{h,H}u_{h,H},$$

which yields the results immediately. \square

3.4. Formulation of FE-LODM

Note that the fine-scale projection Q_h in (3.5) is defined globally onto $W_{0,h}$, and consequently, in order to calculating the basis functions of the discrete space $V_{h,H}^{ms}$, one has to solve many large equations with $\dim(W_{0,h})$ unknowns.

Therefore, for practical application, we have to localize the definition of Q_h to obtain an approximation of the ideal combined multiscale method, i.e., FE-LODM. To do so, we first decompose Q_h by restrict (3.5) to each elements in $\mathcal{M}_{h,H}$ and then localize the restrictions.

For each $T \in \mathcal{M}_{H,\Omega_2}$ we associate it with a point set $\tilde{T} \supseteq T$ defined as follows. If $T \in \mathcal{M}_{H,\Omega_2} \setminus \mathcal{M}_{\Gamma_H}$, we just let $\tilde{T} = T$. While, for $T \in \mathcal{M}_{\Gamma_H}$, we let

$$\tilde{T} := T \cup \{t \in \mathcal{M}_{\Gamma_h} : (t \cap \Gamma) \subset (T \cap \Gamma)\}$$

be the union of T and those interface elements in \mathcal{M}_{Γ_h} whose intersections with the interface Γ are contained in ∂T (see Figure 2 for an illustration).

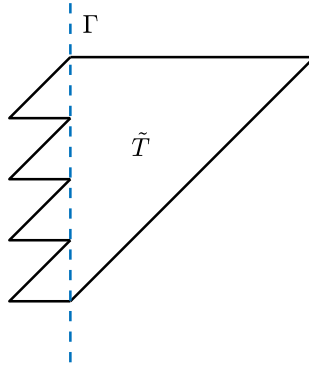


Figure 2: An illustration of the interface combined element \tilde{T} for $T \in \mathcal{M}_{\Gamma_H}$.

240

Then we define the restrictions of Q_h for any $T \in \mathcal{M}_{H,\Omega_2}$ as: $Q_h^T v_{h,h} \in W_{0,h}$ such that

$$a_\Omega(Q_h^T v_{h,h}, w_{0,h}) = a_{\tilde{T}}(v_{h,h}, w_{0,h}) \quad \forall w_{0,h} \in W_{0,h}. \quad (3.12)$$

Remark 3. For $v_{h,h} \in V_{h,h}, w_{0,h} \in W_{0,h}$, $a_\Omega(v_{h,h}, w_{0,h})$ has nonzero terms on the interface Γ_h . We integrate them into the definition of $Q_h^T v_{h,h}$ for the elements $T \in \mathcal{M}_{\Gamma_H}$ by restricting the bilinear form a onto \tilde{T} .

Noting that any function in $W_{0,h}$ vanishes in Ω_1 , from (2.5) we have

$$a_{\Omega_1 \setminus (\cup_{T \in \mathcal{M}_{\Gamma_h}} T)}(v_{h,h}, w_{0,h}) = 0 \quad \forall v_{h,h} \in V_{h,h}, w_{0,h} \in W_{0,h}.$$

Therefore it follows from (3.5) that

$$a_\Omega(Q_h v_{h,h}, w_{0,h}) = \sum_{T \in \mathcal{M}_{H,\Omega_2}} a_{\tilde{T}}(v_{h,h}, w_{0,h}) \quad \forall w_{0,h} \in W_{0,h},$$

and hence we have the following decomposition:

$$Q_h = \sum_{T \in \mathcal{M}_{H,\Omega_2}} Q_h^T. \quad (3.13)$$

Although the definitions of $Q_h^T v_{h,H}$ are independent of each other and can
 245 be computed in parallel, they are still global and have to be solved on the whole
 fine-scale space $W_{0,h}$.

Next we introduce local versions of the correction operators Q_h^T and give
 error estimates between them. To this end, we need the definitions of element
 patches (c.f. [21]).

Definition 1 (element patches). *Given $T \in \mathcal{M}_{H,\Omega_2}$, the patches T_L are defined
 recursively as follows:*

$$\begin{aligned} T_0 &:= T, \\ T_L &:= \{T' \in \mathcal{M}_{H,\Omega_2} \mid T' \cap T_{L-1} \neq \emptyset\} \quad L = 1, 2, \dots \end{aligned}$$

The restriction of the fine-scale correction space $W_{0,h}$ to the element patch
 T_L is defined by

$$W_{0,h}(T_L) := \{v_{h,h} \in W_{0,h} : v_{h,h} = 0 \text{ in } \Omega \setminus T_L\}.$$

250 The localized approximation of the correction operator Q_h^T is defined as follows.

Definition 2. *For $T \in \mathcal{M}_{H,\Omega_2}$ and the patch T_L , the local correction operator
 $Q_h^{T,L} : V_{h,h} \mapsto W_{0,h}(T_L)$ is defined as follows: given $v_{h,h} \in V_{h,h}$, find $Q_h^{T,L} v_{h,h}$
 $\in W_{0,h}(T_L)$ such that*

$$a_\Omega(Q_h^{T,L} v_{h,h}, w_{0,h}) = a_{\bar{T}}(v_{h,h}, w_{0,h}) \quad \forall w_{0,h} \in W_{0,h}(T_L). \quad (3.14)$$

According to the decomposition (3.13) and the above definition, the global
 corrector of level L is given by

$$Q_h^L := \sum_{T \in \mathcal{M}_{H,\Omega_2}} Q_h^{T,L}. \quad (3.15)$$

Further, we define the localized multiscale approximation space as follows:

$$V_{h,H}^{ms,L} := (I - Q_h^L) V_{h,H} = \{v_{h,H} - Q_h^L v_{h,H} : v_{h,H} \in V_{h,H}\}. \quad (3.16)$$

Then, the FE-LODM reads as: find $u_{h,H}^{ms,L} \in V_{h,H}^{ms,L}$, such that

$$a_{\Omega}(u_{h,H}^{ms,L}, v_{h,H}^{ms,L}) = (f, v_{h,H}^{ms,L}) \quad \forall v_{h,H}^{ms,L} \in V_{h,H}^{ms,L}. \quad (3.17)$$

Remark 4. (1) *It is clear that $V_{h,H}^{ms,L} \subset V_{h,h}$ as a consequence of the assumption that \mathcal{M}_{h,Ω_2} is a refinement of \mathcal{M}_{H,Ω_2} . Therefore the FE-LODM inherits the well-posedness from the reference problem (2.7).*

(2) *Unlike $V_{h,H}^{ms}$ whose multiscale basis functions supported globally on Ω_2 , the multiscale basis functions of $V_{h,H}^{ms,L}$ locally support on small patches of size $O(LH)$, and hence the computational cost for assembling the global system of the FE-LODM (3.17) is usually much less than that for the ideal combined method (3.7).*

4. Error estimates for the FE-LODM

In this section, we derive the H^1 and L^2 error estimates for the proposed FE-LODM.

We first recall two local trace inequalities which will be used in this paper frequently. Here we omitted the proof since it is a direct consequence of the standard trace inequality (cf. [56, Theorem 1.6.6, p.39]) and the scaling argument (cf. [60]).

Lemma 4.1. *Let T be an element in the triangulation \mathcal{M}_{h,Ω_1} , \mathcal{M}_{h,Ω_2} , or \mathcal{M}_{H,Ω_2} . Then, we have*

$$\begin{aligned} \|v\|_{0,\partial T} &\lesssim \text{diam}(T)^{-\frac{1}{2}} \|v\|_{0,T} + \|v\|_{0,T}^{\frac{1}{2}} \|\nabla v\|_{0,T}^{\frac{1}{2}} \quad \forall v \in H^1(T), \\ \|v\|_{0,\partial T} &\lesssim \text{diam}(T)^{-\frac{1}{2}} \|v\|_{0,T} \quad \forall v \in P_1(T), \end{aligned}$$

where the invisible constants depend only on the regularity of the element T .

We shall also make use of the following norm on the restriction of the space $V_{h,H}$ onto a subdomain $\omega \subseteq \Omega$:

$$\|v\|_{h,H,\omega} = \left(\|A^{\frac{1}{2}} \nabla_h v\|_{0,\omega}^2 + \frac{\gamma_0}{H} \|[v]\|_{\Gamma \cap \omega}^2 \right)^{\frac{1}{2}}, \quad (4.1)$$

and denote by $\|\cdot\|_{h,H} := \|\cdot\|_{h,H,\Omega}$. Note that the norm $\|\cdot\|_{h,H,\omega}$ is almost the same as the previous one $\|\cdot\|_{h,h,\omega}$ in (2.10) except replacing $\frac{\gamma_0}{h}$ there by $\frac{\gamma_0}{H}$.

4.1. Properties of the operator $\mathcal{C}_{h,H}$

270 In this subsection, we state two lemmas on the quasi-interpolation operator $\mathcal{C}_{h,H}$ given in (3.3).

First we recall some stability and error estimates for the operator \mathcal{C}_H , whose proof can be found in [58, 59].

Lemma 4.2. *For any $T \in \mathcal{M}_{H,\Omega_2}$ and $v_h \in V_{h,\Omega_2}$, there hold following estimates*

$$\|\nabla_h \mathcal{C}_H v_h\|_{0,T} \lesssim \|\nabla_h v_h\|_{0,\hat{T}}, \quad (4.2)$$

$$\|v_h - \mathcal{C}_H v_h\|_{0,T} + H \|\nabla_h(v_h - \mathcal{C}_H v_h)\|_{0,T} \lesssim H \|\nabla_h v_h\|_{0,\hat{T}}, \quad (4.3)$$

where $\hat{T} = \cup\{T' \in \mathcal{M}_{H,\Omega_2} : T' \cap T \neq \emptyset\}$.

275 Using Lemma 4.2, we may prove the following stability result for $\mathcal{C}_{h,H}$.

Lemma 4.3. *For any $v_{h,h} \in V_{h,h}$, it holds that*

$$\|\mathcal{C}_{h,H} v_{h,h}\|_{h,H,\omega} \lesssim \|v_{h,h}\|_{h,H,\hat{\omega}}, \quad (4.4)$$

where $\hat{\omega} := \cup(\{\hat{T} : T \cap \omega \neq \emptyset, T \in \mathcal{M}_{H,\Omega_2}\} \cup \{T : T \cap \omega \neq \emptyset, T \in \mathcal{M}_{h,\Omega_1}\})$.

Proof. From the definitions (2.10) and (4.1) of the norms, (3.2), (3.3), and (4.2), it is easy to see that

$$\begin{aligned} \|\mathcal{C}_{h,H} v_{h,h}\|_{h,H,\omega}^2 &\lesssim \sum_{T \in \mathcal{M}_{H,\Omega_2} \cap \omega} \|A^{\frac{1}{2}} \nabla_h v_{h,h}\|_{0,\hat{T}}^2 \\ &\quad + \|A^{\frac{1}{2}} \nabla_h v_{h,h}\|_{0,\Omega_1 \cap \omega}^2 + \frac{\gamma_0}{H} \|\mathcal{C}_{h,H} v_{h,h}\|_{\Gamma \cap \omega}^2 \\ &\lesssim \|A^{\frac{1}{2}} \nabla_h v_{h,h}\|_{0,\Omega \cap \hat{\omega}}^2 + \frac{\gamma_0}{H} \|\mathcal{C}_{h,H} v_{h,h}\|_{\Gamma \cap \omega}^2. \end{aligned} \quad (4.5)$$

For the second term on the right hand side, using the triangle inequality, we have

$$\begin{aligned} \frac{\gamma_0}{H} \|\mathcal{C}_{h,H} v_{h,h}\|_{\Gamma \cap \omega}^2 &\lesssim \frac{\gamma_0}{H} \|\mathcal{C}_{h,H} v_{h,h} - v_{h,h}\|_{\Gamma \cap \omega}^2 + \frac{\gamma_0}{H} \|[v_{h,h}]\|_{\Gamma \cap \omega}^2 \\ &\lesssim \sum_{\substack{E \in \Gamma_H \\ E \cap \omega \neq \emptyset}} \frac{\gamma_0}{H} \|\mathcal{C}_H v_{h,\Omega_2} - v_{h,\Omega_2}\|_E^2 + \frac{\gamma_0}{H} \|[v_{h,h}]\|_{\Gamma \cap \omega}^2 \\ &:= \text{I} + \frac{\gamma_0}{H} \|[v_{h,h}]\|_{\Gamma \cap \omega}^2, \end{aligned} \quad (4.6)$$

where $v_{h,\Omega_2} := v_{h,h}|_{\Omega_2}$, and we have used the fact that $\mathcal{C}_{h,H}v_{h,h}|_{\Omega_1} = v_{h,h}|_{\Omega_1}$.

Further, from Lemma 4.1 and (4.3), it follows that

$$\begin{aligned} \text{I} &\lesssim \sum_{\substack{T \in \mathcal{M}_{\Gamma_H} \\ T \cap \omega \neq \emptyset}} \frac{\gamma_0}{H} (H^{-1} \|\mathcal{C}_H v_{h,\Omega_2} - v_{h,\Omega_2}\|_{0,T}^2 + H \|\nabla_h(\mathcal{C}_H v_{h,\Omega_2} - v_{h,\Omega_2})\|_{0,T}^2) \\ &\lesssim \sum_{\substack{T \in \mathcal{M}_{\Gamma_H} \\ T \cap \omega \neq \emptyset}} \|\nabla_h v_{h,\Omega_2}\|_{0,\hat{T}}^2, \end{aligned}$$

which together with (4.5) and (4.6) yields the result immediately. \square

The following lemma gives a stability estimate of $\mathcal{C}_{h,H}|_{V_{h,H}}$, whose proof is arranged in Appendix A for the convenience of the reader.

Lemma 4.4. $\mathcal{C}_{h,H}$ is an isomorphism on $V_{h,H}$ and satisfies the following estimate

$$\|(\mathcal{C}_{h,H}|_{V_{h,H}})^{-1} v_{h,H}\|_{h,H} \lesssim \|v_{h,H}\|_{h,H} \quad \forall v_{h,H} \in V_{h,H}.$$

The following lemma is crucial for the error analysis, which can be proved by following the proof of [19, Lemma 2.1] or [49, Lemma 1]. We omit the details.

Lemma 4.5. For each $v_{0,H} \in V_{0,H}$, there exists a $v_{0,h} \in V_{0,h}$, such that $\mathcal{C}_{h,H}v_{0,h} = v_{0,H}$, $\|v_{0,h}\|_{h,h} \lesssim \|v_{0,H}\|_{h,H}$ and $\text{supp } v_{0,h} \subseteq \text{supp } (\mathcal{C}_{h,H}v_{0,H})$.

We emphasize that the above result holds for any function in $V_{0,H}$, not $V_{h,H}$, which is sufficient for the later analysis. In fact, we have tried to use $V_{h,H}$ instead of $V_{0,H}$, but the error estimate has become worse, multiplying by an additional factor H/h .

4.2. Error estimate for the ideal combined multiscale method

The following theorem gives an error bound for the ideal multiscale method (3.7), where the correctors for the basis functions have to be solved globally (see (3.5) and (3.6)). The proposed ideal combined multiscale method preserves the common linear order convergence $O(H)$ for the H^1 -error without suffering from preasymptotic effects due to the highly varying diffusion coefficient.

Theorem 4.1. *If $u_{h,h}$ and $u_{h,H}^{ms}$ are the solutions of the reference problem (2.7) and the approximation problem (3.7) respectively, then it holds that*

$$\|u_{h,h} - u_{h,H}^{ms}\|_{h,h} \lesssim H \|f\|_{L^2(\Omega)}. \quad (4.7)$$

Proof. Let $e_h = u_{h,h} - u_{h,H}^{ms}$. From Proposition 1 we have $e_h \in W_{0,h}$. Hence $C_{h,H}e_h = 0$. Thus, using the Cauchy-Schwarz inequality and the coercivity (2.9) of a_Ω on $V_{h,h}$, we have

$$\begin{aligned} \|e_h\|_{h,h}^2 &\lesssim a_\Omega(e_h, e_h) = (f, e_h) = (f, e_h - C_{h,H}e_h) \\ &\leq \|f\|_{L^2(\Omega)} \|e_h - C_{h,H}e_h\|_{L^2(\Omega)} \\ &= \|f\|_{L^2(\Omega)} \sum_{T \in \mathcal{M}_{H,\Omega_2}} \|e_h - C_H e_h\|_{0,T}. \end{aligned}$$

Further, from (4.3), it follows that

$$\sum_{T \in \mathcal{M}_{H,\Omega_2}} \|e_h - C_H e_h\|_{0,T} \lesssim \sum_{T \in \mathcal{M}_{H,\Omega_2}} H \|\nabla e_h\|_{0,\hat{T}} \lesssim H \|e_h\|_{h,h},$$

295 which combines the above estimate yields the result immediately. \square

4.3. Error estimates for the localized method

In this subsection we first estimate the errors between the correctors Q_h^T and $Q_h^{T,L}$ due to the truncations to local patches. Then we provide H^1 - and L^2 -error bounds for the FE-LODM.

We will frequently make use of the following cut-off functions on element patches: for each $T \in \mathcal{M}_{H,\Omega_2}$ and $l_1 < l_2 \in \mathbb{N}$, the cut-off functions $\eta_T^{l_1, l_2} \in V_{h,H}$ satisfy

$$\eta_T^{l_1, l_2}|_{T_{l_1}} = 1, \quad (4.8)$$

$$\eta_T^{l_1, l_2}|_{\Omega \setminus T_{l_2}} = 0, \quad (4.9)$$

$$\|\nabla_h \eta_T^{l_1, l_2}\|_{L^\infty(\Omega)} \lesssim \frac{1}{(l_2 - l_1)H_T}. \quad (4.10)$$

300 Let $I_{h,h}$ ($I_{h,h}|_{\Omega_i} : H_{\Gamma_i}^1(\Omega_i) \cap C(\bar{\Omega}_i) \mapsto V_{h,\Omega_i}, i = 1, 2$) be the linear Lagrange interpolation operator with respect to $\mathcal{M}_{h,h}$. The following lemma provides a stability estimate of the operator $I_{h,h}$.

Lemma 4.6. For $T \in \mathcal{M}_{H,\Omega_2}$, assume that $\eta_T^{s,n}$, $n > s > 0 \in \mathbb{N}$ is the cut-off function which satisfies (4.8)–(4.10). Then for $w \in W_{0,h}$, the following estimates hold

$$\|I_{h,h}(\eta_T^{s,n}w)\|_{h,h} \lesssim \|w\|_{h,h,T_{n+1}}, \quad (4.11)$$

$$\|\eta_T^{s,n}w - I_{h,h}(\eta_T^{s,n}w)\|_{h,h} \lesssim \|w\|_{h,h,T_{n+1} \setminus T_{s-1}}, \quad (4.12)$$

$$\|I_{h,h}(\eta_T^{s,n}w)\|_{h,h,T_n \setminus T_s} \lesssim \|w\|_{h,h,T_{n+1} \setminus T_{s-1}}, \quad (4.13)$$

$$\|I_{h,h}(1 - \eta_T^{s,n})w\|_{h,h} \lesssim \|w\|_{h,h,\Omega \setminus T_{s-1}}. \quad (4.14)$$

The proof of this lemma is similar to that of [21, Lemma A.2], except that we have to deal with the elements near the interface between coarse and fine meshes. For convenience of the reader, we arrange it in Appendix B.

The following key lemma says that the errors of the localized correction problems decay exponentially with respect to the number of truncation layers L .

Lemma 4.7. Let $u_{h,h}$ be the reference solution to (2.7) and $u_{h,H}^{ms} \in V_{h,H}^{ms}$ be the ideal solution to (3.7), respectively. Denote by $u_{h,H} = (\mathcal{C}_{h,H}|_{V_{h,H}})^{-1}\mathcal{C}_{h,H}u_{h,H}^{ms} \in V_{h,H}$. Further, for $T \in \mathcal{M}_{H,\Omega_2}$ and its element patch T_L , let $q_h^T = Q_h^T(u_{h,H})$ and $q_h^{T,L} = Q_h^{T,L}(u_{h,H})$ be the global and local multiscale-corrected solution obtained in (3.12) and (3.14), respectively. Then there exists a constant $0 < \theta < 1$ independent of L, h, H , and T , such that

$$\|q_h^T - q_h^{T,L}\|_{h,h} \lesssim \theta^L \|u_{h,H}\|_{h,h,\tilde{T}},$$

where \tilde{T} is defined in Section 3.4.

The proof of this lemma is similar to that given in [19] and [21], but with some special details related to the interface elements need to be accounted for. To make the error analysis clearer, we arrange the proof of this lemma in Appendix C.

The following theorem gives the H^1 -error estimate for the FE-LODM. Using this theorem, we can quantify how many truncation layers in the localization patches can ensure the linear convergence of $O(H)$.

Theorem 4.2. *Suppose $\gamma_0 \geq \alpha_0$. Let $u_{h,h}$ and $u_{h,H}^{ms,L}$ be the reference solution to (2.7) and the solution to the FE-LODM (3.17), respectively. Then we have*

$$\|u_{h,h} - u_{h,H}^{ms,L}\|_{h,h} \lesssim H \|f\|_{L^2(\Omega)} + \left(\frac{H}{h}\right)^{\frac{1}{2}} L^{\frac{\theta}{2}} \theta^L \|f\|_{L^2(\Omega)}, \quad (4.15)$$

where $0 < \theta < 1$ is given in Lemma 4.7. Moreover, there exists a positive constant L_0 such that when $L \geq L_0 |\log(Hh)^{\frac{1}{2}}|$, we have the following estimate, which is of the same order as the ideal multiscale method,

$$\|u_{h,h} - u_{h,H}^{ms,L}\|_{h,h} \lesssim H \|f\|_{L^2(\Omega)}. \quad (4.16)$$

Proof. Let $u_{h,H}^{ms} \in V_{h,H}^{ms}$ be the solution to the ideal method (3.7) using the global basis. From (3.9) and (3.13), the ideal solution can be rewritten as follows:

$$u_{h,H}^{ms} = u_{h,H} - \sum_{T \in \mathcal{M}_{H,\Omega_2}} Q_h^T(u_{h,H}),$$

where $u_{h,H} = (\mathcal{C}_{h,H}|_{V_{h,H}})^{-1} \mathcal{C}_{h,H} u_{h,H}^{ms} \in V_{h,H}$. Denote by

$$\begin{aligned} \tilde{u}_{h,H}^{ms,L} &:= u_{h,H} - \sum_{T \in \mathcal{M}_{H,\Omega_2}} Q_h^{T,L}(u_{h,H}), \\ z &:= \sum_{T \in \mathcal{M}_{H,\Omega_2}} (Q_h^T(u_{h,H}) - Q_h^{T,L}(u_{h,H})). \end{aligned}$$

It is easy to see that

$$\|u_{h,H}^{ms} - \tilde{u}_{h,H}^{ms,L}\|_{h,h} = \|z\|_{h,h}. \quad (4.17)$$

According to Lemma 4.5 with $v_{0,H} = \mathcal{C}_{h,H} I_{h,h}(z - \eta_T^{L+2,L+3} z)$, there exists a function $b \in V_{0,h}$ such that

$$\mathcal{C}_{h,H}(b) = \mathcal{C}_{h,H} I_{h,h}(z - \eta_T^{L+2,L+3} z), \quad (4.18)$$

$$\|b\|_{h,h} \lesssim \|\mathcal{C}_{h,H} I_{h,h}(z - \eta_T^{L+2,L+3} z)\|_{h,H} = \|\mathcal{C}_{h,H} I_{h,h}(\eta_T^{L+2,L+3} z)\|_{h,H}, \quad (4.19)$$

where we have used $\mathcal{C}_{h,H} I_{h,h} z = 0$ to derive the last equality, which is a consequence of the fact that $z \in W_{0,h}$. From (4.9), we have

$$\mathcal{C}_{h,H} I_{h,h}(z - \eta_T^{L+2,L+3} z) = -\mathcal{C}_{h,H} I_{h,h}(\eta_T^{L+2,L+3} z) = 0 \quad \text{in } \Omega \setminus T_{L+4},$$

which together with Lemma 4.5, implies that

$$\text{supp}(b) \subseteq \text{supp}(\mathcal{C}_{h,H}^2 I_{h,h}(z - \eta_T^{L+2,L+3} z)) \subseteq T_{L+5} \setminus T_L.$$

Therefore, from (4.18), we have $I_{h,h}(z - \eta_T^{L+2,L+3}z) - b \in W_{0,h}$. Hence, from (3.12) it follows that

$$a_\Omega(Q_h^T u_{h,H}, I_{h,h}(z - \eta_T^{L-3,L-2}z) - b) = a_{\bar{T}}(u_{h,H}, I_{h,h}(z - \eta_T^{L+2,L+3}z) - b) = 0. \quad (4.20)$$

Further, from $\text{supp}(I_{h,h}(z - \eta_T^{L+2,L+3}z) - b) \subset \Omega_2 \setminus T_L$, it follows that

$$a_\Omega(Q_h^{T,L} u_{h,H}, I_{h,h}(z - \eta_T^{L+2,L+3}z) - b) = 0,$$

which combines with (4.20) yields

$$a_\Omega((Q_h^T - Q_h^{T,L})u_{h,H}, z - I_{h,h}(\eta_T^{L+2,L+3}z) - b) = 0. \quad (4.21)$$

Therefore, from (2.9), it follows that

$$\begin{aligned} \|z\|_{h,h}^2 &\lesssim a_\Omega(z, z) \\ &= \sum_{T \in \mathcal{M}_{H,\Omega_2}} a_\Omega(Q_h^T u_{h,H} - Q_h^{T,L} u_{h,H}, z) \\ &= \sum_{T \in \mathcal{M}_{H,\Omega_2}} a_\Omega((Q_h^T - Q_h^{T,L})u_{h,H}, I_{h,h}(\eta_T^{L+2,L+3}z) + b). \end{aligned}$$

Further, using (4.19) and Lemmas 4.3 and 4.6, we obtain

$$\begin{aligned} \|z\|_{h,h}^2 &\lesssim \sum_{T \in \mathcal{M}_{H,\Omega_2}} \|(Q_h^T - Q_h^{T,L})u_{h,H}\|_{h,h} (\|I_{h,h}(\eta_T^{L+2,L+3}z)\|_{h,h} + \|b\|_{h,h}) \\ &\lesssim \sum_{T \in \mathcal{M}_{H,\Omega_2}} \|(Q_h^T - Q_h^{T,L})u_{h,H}\|_{h,h} \|I_{h,h}(\eta_T^{L+2,L+3}z)\|_{h,h} \\ &\lesssim \sum_{T \in \mathcal{M}_{H,\Omega_2}} \|(Q_h^T - Q_h^{T,L})u_{h,H}\|_{h,h} \|z\|_{h,h,T_{L+4}}. \end{aligned}$$

Thus, by use of the Cauchy-Schwarz inequality, we have

$$\begin{aligned} \|z\|_{h,h}^2 &\lesssim \left(\sum_{T \in \mathcal{M}_{H,\Omega_2}} \|(Q_h^T - Q_h^{T,L})u_{h,H}\|_{h,h}^2 \right)^{\frac{1}{2}} \left(\sum_{T \in \mathcal{M}_{H,\Omega_2}} \|z\|_{h,h,T_{L+4}}^2 \right)^{\frac{1}{2}} \\ &\lesssim \left(\sum_{T \in \mathcal{M}_{H,\Omega_2}} \|(Q_h^T - Q_h^{T,L})u_{h,H}\|_{h,h}^2 \right)^{\frac{1}{2}} \left(L^{\frac{d}{2}} \|z\|_{h,h} \right), \end{aligned}$$

which yields

$$\|z\|_{h,h}^2 \lesssim L^d \sum_{T \in \mathcal{M}_{H,\Omega_2}} \|(Q_h^T - Q_h^{T,L})u_{h,H}\|_{h,h}^2.$$

According to Lemma 4.7, we have

$$\|z\|_{h,h}^2 \lesssim L^d \theta^{2L} \sum_{T \in \mathcal{M}_{H,\Omega_2}} \|u_{h,H}\|_{h,h,\tilde{T}}^2 \lesssim L^d \theta^{2L} \|u_{h,H}\|_{h,h}^2.$$

Moreover, from Lemmas 4.4 and 4.3 and the stability estimate (3.8) of $u_{h,H}^{ms}$, we have

$$\begin{aligned} \|u_{h,H}\|_{h,h}^2 &\lesssim \frac{H}{h} \|u_{h,H}\|_{h,H}^2 = \frac{H}{h} \|(\mathcal{C}_{h,H}|_{V_{h,H}})^{-1} \mathcal{C}_{h,H} u_{h,H}^{ms}\|_{h,H}^2 \\ &\lesssim \frac{H}{h} \|\mathcal{C}_{h,H} u_{h,H}^{ms}\|_{h,H}^2 \lesssim \frac{H}{h} \|u_{h,H}^{ms}\|_{h,H} \lesssim \frac{H}{h} \|f\|_{L^2(\Omega)}. \end{aligned}$$

Thus,

$$\|z\|_{h,h} \lesssim \left(\frac{H}{h}\right)^{\frac{1}{2}} L^{\frac{d}{2}} \theta^L \|f\|_{L^2(\Omega)}. \quad (4.22)$$

Noting that $V_{h,H}^{ms,L} \subseteq V_{h,h}$, from the continuity and coercivity of a_Ω (2.8)–(2.9), we have the following estimate of Céa lemma type:

$$\|u_{h,h} - u_{h,H}^{ms,L}\|_{h,h} \lesssim \inf_{v_{h,H}^{ms,L} \in V_{h,H}^{ms,L}} \|u_{h,h} - v_{h,H}^{ms,L}\|_{h,h},$$

which implies that

$$\|u_{h,h} - u_{h,H}^{ms,L}\|_{h,h} \lesssim \|u_{h,h} - \tilde{u}_{h,H}^{ms,L}\|_{h,h}.$$

Thus, we have

$$\begin{aligned} \|u_{h,h} - u_{h,H}^{ms,L}\|_{h,h} &\leq \|u_{h,h} - u_{h,H}^{ms}\|_{h,h} + \|u_{h,H}^{ms} - \tilde{u}_{h,H}^{ms,L}\|_{h,h} \\ &= \|u_{h,h} - u_{h,H}^{ms}\|_{h,h} + \|z\|_{h,h}, \end{aligned} \quad (4.23)$$

which combines (4.7) and (4.22) yields the estimate (4.15) immediately.

It remains to prove (4.16). Let $\theta_1 = \frac{1+\theta}{2}$. Noting that $L^{\frac{d}{2}} \theta^L \lesssim \theta_1^L$, we have

$$\left(\frac{H}{h}\right)^{\frac{1}{2}} L^{\frac{d}{2}} \theta^L \lesssim \left(\frac{H}{h}\right)^{\frac{1}{2}} \theta_1^L \lesssim H, \quad \text{if } L \geq \frac{|\log(Hh)^{\frac{1}{2}}|}{|\log \theta_1|},$$

which implies that (4.16) holds. This completes the proof of the theorem. \square

Remark 5. (1) If $h = H^m$ for some constant $m > 1$, then $|\log(Hh)^{\frac{1}{2}}| \approx$
320 $|\log H|$, and hence the condition $L \geq L_0 |\log(Hh)^{\frac{1}{2}}|$ becomes $L \geq L'_0 |\log H|$ for some sufficiently large constant L'_0 . Note that this is a standard condition for LOD type methods [19, 21, 47].

(2) In the case where $h = H^3$, it is easy to see that $\sqrt{\frac{H}{h}} = H^{-1}$. Hence (4.15) becomes

$$\|u_{h,h} - u_{h,H}^{ms,L}\|_{h,h} \lesssim H\|f\|_{L^2(\Omega)} + H^{-1}L^{\frac{d}{2}}\theta^L\|f\|_{L^2(\Omega)}, \quad (4.24)$$

which is the same result as those of the methods mentioned in [19, 48, 47]. We emphasize that in our later numerical experiments, we choose $h = H^m$ for some constant $1 < m < 3$, which follows that $\sqrt{\frac{H}{h}} < H^{-1}$. This means in this case the estimate (4.15) is better than (4.24).

The following theorem gives the L^2 error estimate of the proposed FE-LODM.

Theorem 4.3. *Suppose $\gamma_0 \geq \alpha_0$. Then we have the following estimate:*

$$\|u_{h,h} - u_{h,H}^{ms,L}\|_{L^2(\Omega)} \lesssim \left(H + \left(\frac{H}{h}\right)^{\frac{1}{2}}L^{\frac{d}{2}}\theta^L\right)^2\|f\|_{L^2(\Omega)}. \quad (4.25)$$

Moreover, there exists a positive constant L_0 such that when $L \geq L_0|\log(Hh)^{\frac{1}{2}}|$, we have the following estimate,

$$\|u_{h,h} - u_{h,H}^{ms,L}\|_{L^2(\Omega)} \lesssim H^2\|f\|_{L^2(\Omega)}. \quad (4.26)$$

Proof. It suffices to prove (4.25). Let $e_h = u_{h,h} - u_{h,H}^{ms,L}$. We consider the dual problem

$$\begin{cases} -\nabla \cdot (A\nabla w) = e_h & \text{in } \Omega, \\ w = 0 & \text{on } \partial\Omega. \end{cases}$$

Let $w_{h,h} \in V_{h,h}$ be the IPCDG approximation of w :

$$a_\Omega(w_{h,h}, \phi_{h,h}) = (e_h, \phi_{h,h}) \quad \forall \phi_{h,h} \in V_{h,h},$$

and let $w_{h,H}^{ms,L} \in V_{h,H}^{ms,L}$ be the FE-LOD approximation of w :

$$a_\Omega(w_{h,H}^{ms,L}, v_{h,H}^{ms,L}) = (e_h, v_{h,H}^{ms,L}) \quad \forall v_{h,H}^{ms,L} \in V_{h,H}^{ms,L}.$$

Further, from (2.7) and (3.17), it follows that

$$a_\Omega(e_h, w_{h,H}^{ms,L}) = 0.$$

Thus from Theorem 4.2 we have

$$\begin{aligned} \|e_h\|_{L^2(\Omega)}^2 &= a_\Omega(w_{h,h}, e_h) = a_\Omega(e_h, w_{h,h} - w_{h,H}^{ms,L}) \\ &\lesssim \|e_h\|_{h,h} \|w_{h,h} - w_{h,H}^{ms,L}\|_{h,h} \\ &\lesssim \|e_h\|_{h,h} \left(H + \left(\frac{H}{h} \right)^{\frac{1}{2}} L^{\frac{d}{2}} \theta^L \right) \|e_h\|_{L^2(\Omega)}, \end{aligned}$$

which yields

$$\|e_h\|_{L^2(\Omega)} \lesssim \|e_h\|_{h,h} \left(H + \left(\frac{H}{h} \right)^{\frac{1}{2}} L^{\frac{d}{2}} \theta^L \right) \lesssim \left(H + \left(\frac{H}{h} \right)^{\frac{1}{2}} L^{\frac{d}{2}} \theta^L \right)^2 \|f\|_{L^2(\Omega)}.$$

This completes the proof of the theorem. \square

330 5. Numerical Tests

In this section, we first numerically study how the size of element patches affects the errors, and then illustrate the ability of the proposed FE-LODM to deal with singularities by solving multiscale elliptic problems with a corner singularity and high-contrast channels and steady flow transporting through highly heterogeneous porous media driven by extraction wells, respectively. For comparison, we also present results of the local orthogonal decomposition method (LODM) in [53] and the combined multiscale finite element method (FE-OMsPGM) introduced in [46]. We use the IPCDG solution $u_{h,h}$ to (2.7) on a very fine mesh as a reference solution. Denote the energy norm by $\|\cdot\|_E := \|\nabla A^{\frac{1}{2}} \cdot\|_{0,\Omega_1 \cup \Omega_2}$. We measure the relative errors of an approximate solution U_h in the L^2 , L^∞ and energy norms respectively as follows:

$$\frac{\|U_h - u_{h,h}\|_{L^2}}{\|u_{h,h}\|_{L^2}}, \quad \frac{\|U_h - u_{h,h}\|_{L^\infty}}{\|u_{h,h}\|_{L^\infty}}, \quad \frac{\|U_h - u_{h,h}\|_E}{\|u_{h,h}\|_E}.$$

5.1. Effect of the size of the element patches

In this subsection we study how the size of element patches affects the errors by simulating the following example.

Example 1. Consider the model problem (2.1) on the unit square $\Omega = (0, 1) \times (0, 1)$ with the source term $f \equiv 1$ and different diffusion coefficients to be specified below. And we set $\Omega_1 = (\frac{1}{4}, \frac{3}{8}) \times (\frac{1}{4}, \frac{3}{8})$ as shown in Figure 3.

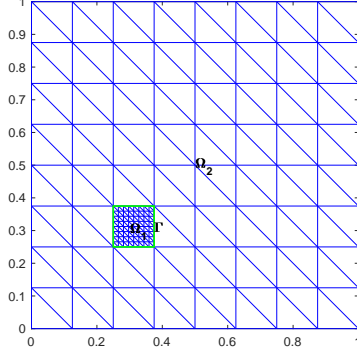


Figure 3: An illustration of the separated domain used in Example 1.

First we test the dependence of the error on the size of the element patches. Consider the following diffusion coefficient:

$$A(x_1, x_2) = \frac{2 + 1.8 \sin(2\pi x_1/\epsilon)}{2 + 1.8 \cos(2\pi x_2/\epsilon)} + \frac{2 + 1.8 \sin(2\pi x_2/\epsilon)}{2 + 1.8 \sin(2\pi x_1/\epsilon)} \quad (5.1)$$

with $\epsilon = 1/5$. We fix $H=2^{-3}$, $h = 2^{-7}$, and let the size of element patches vary. Table 1 shows the relative errors in the energy and L^2 norms on Ω and Ω_1 between the reference solution $u_{h,h}$ and the FE-LOD solution $u_{h,H}^{ms,L}$ with $L = 1, 2, 3, 6, 10$ and the ideal solution $u_{h,H}^{ms}$ as well, respectively. It is observed

Table 1: Example 1: Relative errors for different L , $h = 2^{-7}$, $H = 2^{-3}$, $\gamma_0=10$.

Error \ L	Error in Ω		Error in Ω_1	
	Energy	L^2	Energy	L^2
1	0.1360e-00	0.2929e-01	0.2580e-01	0.1429e-01
2	0.7361e-01	0.1127e-01	0.5881e-02	0.1371e-02
3	0.5712e-01	0.8685e-02	0.1453e-02	0.1712e-03
6	0.5534e-01	0.8625e-02	0.2586e-04	0.6106e-05
10	0.5509e-01	0.8570e-02	0.5213e-06	0.1604e-06
ideal solution	0.5509e-01	0.8569e-02	0.5984e-13	0.2713e-13

that the larger the parameter L , the smaller the relative errors in the energy and L^2 norms on Ω , and tends the errors of the ideal solution, respectively. This observation verifies the estimate in Theorem 4.2. We also notice that the errors of the FE-LOD solution on Ω_1 decrease very quickly as L increases. Especially, in the ideal case, the errors on Ω_1 are almost equal to zero, which is coincided with the result stated in Proposition 1.

Secondly, we study how to choose the size (L) of the element patches to achieve the satisfied approximation behaviour for different coarse-fine grid elements. Recall that in Theorem 4.2, to balance the error between the terms on the right-hand side of (4.15), it is required that the localization parameter L satisfies $L \geq L_0 |\log(Hh)^{\frac{1}{2}}|$ for some positive constant L_0 . Hence, in the following experiments, we choose $L = \lceil L_0 |\log(Hh)^{\frac{1}{2}}| \rceil$ for different constants L_0 . We adopt uniform coarse meshes with sizes $H = 2^{-i}$, $i = 2, 3, 4, 5$, and choose the fine scale reference mesh with size $h = 2^{-9}$, which can resolve the multiscale feature of A . The first test is done for the periodic diffusion coefficient defined in (5.1) with $\epsilon = 1/20$, which is denoted by A_1 for convenience.

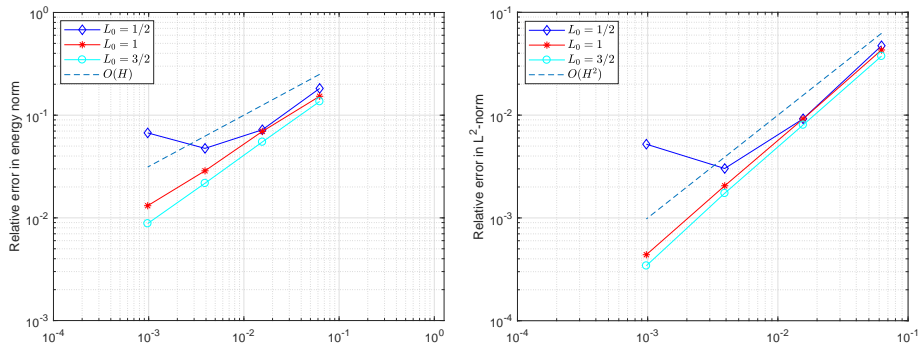


Figure 4: Example 1 with diffusion coefficient $A_1(x)$: Relative errors in energy-norm (left) and L^2 -norm (right) against the size of coarse mesh for $L_0 = 1/2, 1$, and $3/2$, respectively.

Figure 4 shows the log-log plots of the relative errors in energy-norm (left) and L^2 -norm (right) against the size of coarse mesh (H) with different constants $L_0 = 1/2, 1, 3/2$, respectively. It is observed that the method with $L_0 = 1/2$ does

360 not performs well for large mesh size H , while when L_0 is taken as 1 or $3/2$, the error between the terms on the right-hand side of estimate in Theorem 4.2 seems to be balanced, and the convergence rate of the energy-norm error maintains as well as that of the L^2 -norm error.

Note that for larger localization parameter L , it costs more computational
 365 effort to compute the corrector functions and cause reduced sparseness in the coarse scale stiffness matrix. Therefore in the remaining numerical experiments we use $L_0 = 1$. In order to further illustrate the reasonability of choosing $L_0 = 1$, we show the relative error results in Figure 5 for three different diffusion coefficients A : A_1 is defined as above; A_2 is taken as the background medium
 370 in Figure 7, which is a piecewise constant function on a Cartesian grid of size 2^{-9} and is periodic in both the x - and y -directions; A_3 is a randomly generated diffusion coefficient using the moving ellipse average technique in [61] with the parameters described in Example 2 below. It can be seen that taking $L \geq |\log(Hh)^{\frac{1}{2}}|$ (i.e. $L_0 = 1$) in the FE-LODM can give the optimal convergence
 375 rates in both energy- and L^2 - norms for all cases, which are the same as those of the ideal combined multiscale method (see Theorems 4.1–4.3).

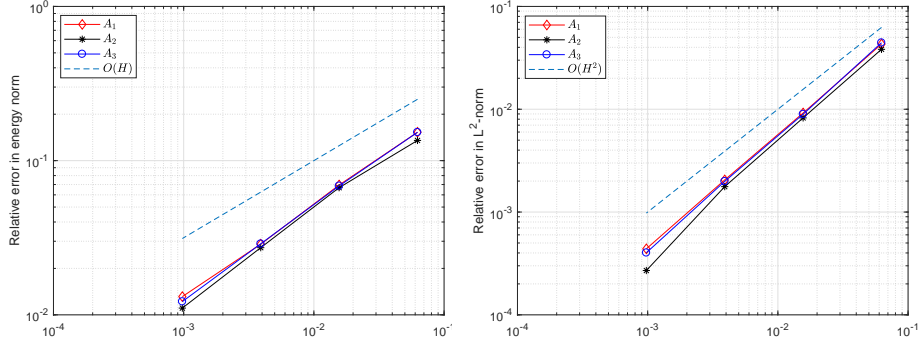


Figure 5: Example 1: Relative errors in energy-norm (left) and L^2 -norm (right) against the size of coarse mesh for $L_0 = 1$ and $A = A_i$, $i = 1, 2, 3$, respectively.

5.2. Application to the multiscale elliptic problem with corner singularity

In this subsection, we consider the following L-shaped domain problem

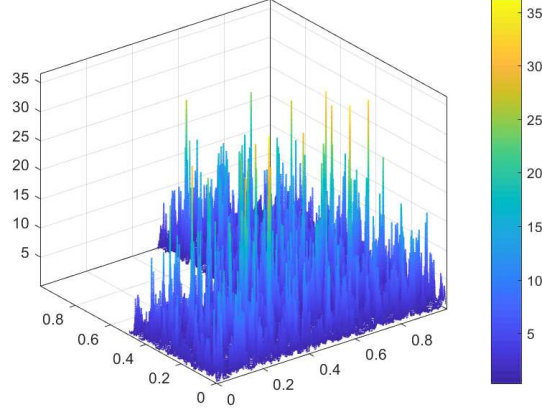


Figure 6: Example 2: The random log-normal permeability field A . $\frac{A_{max}}{A_{min}}=2.9642e+03$.

Example 2. The multiscale problem (2.1) on the L-shaped domain $\Omega = ((0, 1) \times$
 380 $(0, 1)) \setminus ((\frac{1}{2}, 1) \times (0, \frac{1}{2}))$ with the random log-normal permeability field A , which
 is generated by using the moving ellipse average technique [61] with the variance
 of the logarithm of the permeability $\sigma^2 = 1.5$, and the correlation lengths $l_1 =$
 $l_2 = 0.01$ (isotropic heterogeneity) in x_1 and x_2 directions, respectively. One
 realization of the resulting permeability field in our numerical experiments is
 385 depicted in Figure 6.

In this example, we set the refined subdomain $\Omega_1 = ((\frac{3}{8}, \frac{5}{8}) \times (\frac{3}{8}, \frac{5}{8})) \setminus ((\frac{1}{2}, \frac{5}{8}) \times$
 $(\frac{3}{8}, \frac{1}{2}))$ to capture the singularity at the reentrant corner, fix $H = 2^{-5}$, $h = 2^{-10}$,
 and choose the parameter $L = \lceil \log \sqrt{|Hh|} \rceil = 3$. We compare the relative errors
 390 of the FE-LOD solution in the L^2 , L^∞ , and energy norms with those of
 the LOD solution and FE-OMsPG [46] solution in the whole domain as well
 as in the refined region Ω_1 . The errors are listed in Table 2. We observe that
 the introduced FE-LODM gives a better approximation than the LOD and FE-
 OMsPG methods. In particular, in the refined region Ω_1 , our method gives
 much better results than the LOD method, which is very useful if one needs
 395 high-accuracy solution in the problematic area.

Table 2: Example 2: Relative errors for the model problem on the L-shaped domain. $h = 2^{-10}$, $H = 2^{-5}$, $\gamma_0=10$.

Method \ Error	Energy norm	L^2	L^∞
LODM	0.2834e-01	0.1553e-02	0.6536e-02
FE-LODM	0.2628e-01	0.1449e-02	0.6526e-02
FE-OMsPGM	0.1045e-00	0.7596e-02	0.2424e-01
LODM (error in Ω_1)	0.1507e-02	0.1695e-02	0.5583e-02
FE-LODM (error in Ω_1)	0.4257e-03	0.4043e-03	0.5018e-03

5.3. Application to the multiscale problem with high-contrast channels

In this subsection we use the FE-LOD method to solve the elliptic multiscale problem with high-contrast channels.

Example 3. *The oscillating coefficient is set as that of [46]. Namely, as shown in Figure 7, we set the high-permeability channels and inclusions with permeability values equal to 10^5 and 8×10^4 respectively, and set the other values as 1.*

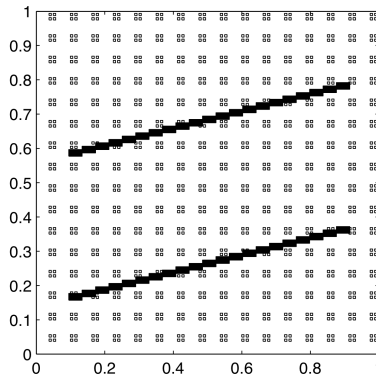


Figure 7: Example 3: Permeability field $A = 10^5$ in two channels consisting of dark small rectangles; $A = 8 \times 10^4$ in small square inclusions; $A = 1$ otherwise.

We set Ω_1 be the union of two layers of coarse-grid elements which contain the channels, fix $h = 2^{-10}$, $H = 2^{-5}$, and choose the parameter $L =$
405 $\lceil \log \sqrt{|Hh|} \rceil = 3$ for this example. The results are listed in Table 3. It is observed that the FE-LOD method performs much better than the other two methods.

Table 3: Example 3: Relative errors for the model problem with the coefficient given by Figure 7. $h = 2^{-10}$, $H = 2^{-5}$, $\gamma_0 = 10$.

Relative error	Energy norm	L^2	L^∞
LODM	0.4938e-01	0.4882e-02	0.1889e-01
FE-LODM	0.2169e-01	0.7238e-03	0.1248e-02
FE-OMsPGM	0.1063e-00	0.5564e-02	0.2580e-00

5.4. Application to the multiscale problem with Dirac singularities

In this subsection, we consider the multiscale problem with singular source
410 terms inside the domain, which originates from the simulation of steady flow transporting through highly heterogeneous porous media driven by extraction wells. This kind of well-singularity problem is of great importance in hydrology, petroleum reservoir engineering, and soil venting techniques.

Denote by $d(P, r)$ the disk centered at point P with radius $r > 0$. We let
415 $\Omega = (0, 1) \times (0, 1)$ and consider two wells $d_j = d(P_j, r)$, $j = 1, 2$ with $P_1(\frac{1}{4}, \frac{3}{4})$, $P_2(\frac{3}{4}, \frac{1}{4})$, and $r = 10^{-5}$. Since the size of the well (radius r) is negligible in situations, we make an approximation to the original single phase pressure equation by the multiscale problem (2.1) with source term $f = \sum_{j=1}^2 q_j \delta_{P_j}$ (c.f. [39]), where q_j is the well flow rate and δ_{P_j} is the Dirac measure at P_j . On
420 the well boundary ∂d_j , two quantities are of particular importance in practical applications: the well bore pressure (WBP) and the well flow rate. Here we fix the well flow rate q_j and try to find the well bore pressure. In the computations we always take $q_1 = -1$ and $q_2 = 1$, which corresponds to the situation that the well d_1 is an extraction well and d_2 is an injection well.

425 In the following two examples, we set Ω_1 be the union of two small squares with edge size of $\frac{1}{16}$ centered at points $P_i, i = 1, 2$. And similarly, we choose the localization parameter $L = \lceil \log \sqrt{|Hh|} \rceil = 3$.

Example 4. *Let the oscillating coefficient A be given by*

$$A(x_1, x_2) = \frac{1}{(2 + 1.5 \sin \frac{2\pi x_1}{\epsilon})(2 + 1.5 \sin \frac{2\pi x_2}{\epsilon})}, \quad (5.2)$$

where we fix $\epsilon = 1/64$.

Since the exact WBPs are unknown, we use the method introduced in [39] 430 to compute them based on the well-resolved solutions obtained on a uniform 2048×2048 mesh. Then we can get the “exact” WBP $\alpha_1 = -5.3884973$ in the first well and $\alpha_2 = 5.3884973$ in the second well (see [39, Example 7.1]).

In addition, we implement three other methods for comparison, including the LODM, the MsFEM introduced in [39, Algorithm 7.1] (referred as G-MsFEM) 435 and the FE-OMsPGM introduced in [46]. The G-MsFEM needs to compute the discrete Green functions in a very fine mesh and it uses the developed new Peaceman method to compute the WBPs (see [39, Section 6]). We also use the new Peaceman method to calculate the WBP on each well for the LOD and FE-LOD method. For FE-OMsPGM, we use the Peaceman model [62] to compute 440 the WBPs since the bilinear form of FE-OMsPG method is nonsymmetric. The results are listed in Table 4. We can see that our FE-LODM provides a better approximation of the WBP than G-MsFEM and FE-OMsPGM, and a much better approximation than the LODM in this example.

Example 5. *We generate the random permeability field A on a uniform $1024 \times$ 445 1024 mesh by using the technique in [61]. Figure 8 shows a realization of the random permeability field.*

Using the same method as above, we can get the “exact” well bore pressures $\alpha_1 = -0.9860407$ and $\alpha_2 = 4.6507306$ by using the fine-grid solution on the 1024×1024 mesh. The results are presented in Table 5. We observe that 450 the proposed FE-LODM gives much better approximation than the other three

Table 4: Example 4: WBPs and relative errors at two wells. $h = 2^{-11}$, $H = 2^{-6}$, $\gamma_0=10$.

Methods	Well no.	WBP	Relative error
G-MsFEM	1	-5.3838442	0.8635e-03
FE-OMsPGM	1	-5.3843102	0.7770e-03
LODM	1	-5.6792672	0.5396e-01
FE-LODM	1	-5.3876085	0.1649e-03
G-MsFEM	2	5.3739254	0.2704e-02
FE-OMsPGM	2	5.3843102	0.7770e-03
LODM	2	5.6792672	0.5396e-01
FE-LODM	2	5.3876085	0.1649e-03

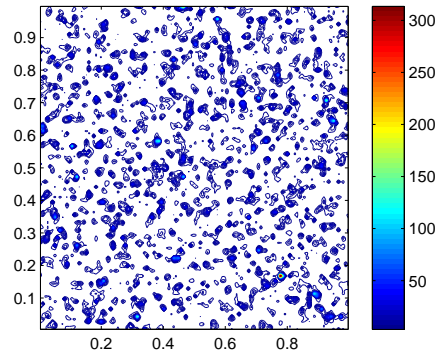


Figure 8: Example 5: The random permeability field A , the ratio of $\frac{A_{max}}{A_{min}}=6.06629e + 003$.

methods, which may be due to the fact that the FE-LODM has more accurate solution near the well than others. This superiority can also be found in the results of FE-OMsPGM, in which the local fine mesh approximation is used in the well-singularity region that is same as that of FE-LODM.

Table 5: Example 5: WBPs and relative errors at two wells. $h = 2^{-10}$, $H = 2^{-6}$, $\gamma_0=10$.

Methods	Well no.	WBP	Relative error
G-MsFEM	1	-0.9478413	0.3874e-01
FE-OMsPGM	1	-0.9701813	0.1608e-01
LODM	1	-0.7536890	0.2356e-00
FE-LODM	1	-0.9864050	0.3695e-03
G-MsFEM	2	1.1477417	0.7532e-00
FE-OMsPGM	2	4.6391148	0.2498e-02
LODM	2	2.8657275	0.3838e-00
FE-LODM	2	4.6591764	0.1816e-02

455 6. Conclusions

In this paper, we have proposed a new combined multiscale method to solve the multiscale elliptic problems which may have singularities. In order to get a good approximation of the solution in the problematic region, we use the traditional FEM directly on a very fine mesh of this subdomain, while in other region
460 where we have a highly oscillating coefficients, we use the multiscale LODM. The key point of implementing this idea is how to define the corrected basis function in the near interface elements. To this end, we introduce a special definition of the cell problems for the elements near the interface. The error analysis is carried out for highly varying coefficients, without any assumption on scale
465 separation or periodicity. Our theoretical and numerical results show that the proposed method is very attractive for multiscale problems with singularities.

Appendix A. Proof of Lemma 4.4

Given $v_H = \sum_{j \in \mathcal{N}_H} v_j \Phi_j \in V_{H, \Omega_2}$, let $w_H := \mathcal{C}_H v_H$. From (3.1) and (3.3), it follows that

$$w_H = \sum_{i \in \mathcal{N}_H} w_i \Phi_i \quad \text{with } w_i = \sum_{j \in \mathcal{N}_H} \frac{(\Phi_i, \Phi_j)_{\Omega_2}}{(1, \Phi_i)_{\Omega_2}} v_j.$$

Denote by $D = \text{diag}((1, \Phi_1)_{\Omega_2}, (1, \Phi_2)_{\Omega_2}, \dots, (1, \Phi_N)_{\Omega_2})$, $M = ((\Phi_i, \Phi_j)_{\Omega_2})_{N \times N}$, $V = (v_i)_{N \times 1}$, $W = (w_i)_{N \times 1}$, where N represents the numbers of vertices in \mathcal{N}_H . Thus we have $D^{-1}MV = W$, which yields

$$V^T MV = V^T DW.$$

Hence, by use of the above equation, it is follows that

$$\begin{aligned} \|v_H\|_{L^2(\Omega)}^2 &= V^T MV \leq |V| |DW| \lesssim H^{-\frac{d}{2}} \|v_H\|_{L^2(\Omega)} H^d |W| \\ &\lesssim \|v_H\|_{L^2(\Omega)} \|w_H\|_{L^2(\Omega)}, \end{aligned}$$

which yields

$$\|v_H\|_{L^2(\Omega)} \lesssim \|w_H\|_{L^2(\Omega)}.$$

Therefore \mathcal{C}_H is an isomorphism on V_{H, Ω_2} and it holds that

$$\|(\mathcal{C}_H|_{V_{H, \Omega_2}})^{-1} w_H\|_{0, \Omega_2} \lesssim \|w_H\|_{0, \Omega_2}. \quad (\text{A.1})$$

Thus, it follows from (3.2) that $\mathcal{C}_{h, H}$ is an isomorphism on $V_{h, H}$. For the sake of simplicity, we denote $(\mathcal{C}_{h, H}|_{V_{h, H}})^{-1}$ by $\mathcal{C}_{h, H}^{-1}$ in the following. From (3.2), it is clear that $\mathcal{C}_{h, H} v_{h, H} - v_{h, H} \in V_{0, H}$. Using the inverse inequality and Lemma 4.1, we have

$$\begin{aligned} \|v_{h, H} - \mathcal{C}_{h, H}^{-1} v_{h, H}\|_{h, H}^2 &= \|\mathcal{C}_{h, H}^{-1} (\mathcal{C}_{h, H} v_{h, H} - v_{h, H})\|_{h, H}^2 \\ &= \|A^{\frac{1}{2}} \nabla ((\mathcal{C}_H|_{V_{H, \Omega_2}})^{-1} (\mathcal{C}_{h, H} v_{h, H} - v_{h, H}))\|_{0, \Omega_2}^2 \\ &\quad + \frac{\gamma_0}{H} \|(\mathcal{C}_H|_{V_{H, \Omega_2}})^{-1} (\mathcal{C}_{h, H} v_{h, H} - v_{h, H})\|_{\Gamma}^2 \\ &\lesssim H^{-2} \|(\mathcal{C}_H|_{V_{H, \Omega_2}})^{-1} (\mathcal{C}_{h, H} v_{h, H} - v_{h, H})\|_{0, \Omega_2}^2. \end{aligned}$$

Further, from (A.1) and (4.3), we have

$$\begin{aligned}
\|v_{h,H} - \mathcal{C}_{h,H}^{-1}v_{h,H}\|_{h,H}^2 &\lesssim H^{-2}\|\mathcal{C}_{h,H}v_{h,H} - v_{h,H}\|_{0,\Omega}^2 \\
&= H^{-2}\sum_{T \in \mathcal{M}_{H,\Omega_2}} \|\mathcal{C}_{h,H}v_{h,H} - v_{h,H}\|_{0,T}^2 \\
&\lesssim \|v_{h,H}\|_{h,H}^2.
\end{aligned}$$

Finally, using triangle inequality, we conclude that

$$\begin{aligned}
\|\mathcal{C}_{h,H}^{-1}v_{h,H}\|_{h,H} &\leq \|\mathcal{C}_{h,H}^{-1}v_{h,H} - v_{h,H}\|_{h,H} + \|v_{h,H}\|_{h,H} \\
&\lesssim \|v_{h,H}\|_{h,H}.
\end{aligned}$$

This completes the proof of the lemma. \square

Appendix B. Proof of Lemma 4.6

We first prove the inequality (4.11). From the interpolation error estimates and the inverse inequality, we have

$$\begin{aligned}
\|\nabla I_{h,h}(\eta_T^{s,n}w)\|_{0,\Omega_2} &\leq \|\nabla I_{h,h}(\eta_T^{s,n}w) - \nabla(\eta_T^{s,n}w)\|_{0,\Omega_2} + \|\nabla(\eta_T^{s,n}w)\|_{0,\Omega_2} \\
&\lesssim \left(\sum_{T \in \mathcal{M}_{h,\Omega_2}} h_T^2 |\eta_T^{s,n}w|_{2,T}^2 \right)^{\frac{1}{2}} + \|\nabla(\eta_T^{s,n}w)\|_{0,\Omega_2} \\
&\lesssim \|\nabla(\eta_T^{s,n}w)\|_{0,\Omega_2}. \tag{B.1}
\end{aligned}$$

Using the triangle inequality, we obtain

$$\begin{aligned}
\|I_{h,h}(\eta_T^{s,n}w)\|_{h,h}^2 &= \|A^{\frac{1}{2}}\nabla I_{h,h}(\eta_T^{s,n}w)\|_{0,\Omega_2}^2 + \sum_{e \in \Gamma_h} \frac{\gamma_0}{h} \|I_{h,h}(\eta_T^{s,n}w)\|_e^2 \\
&\lesssim \|A^{\frac{1}{2}}\nabla(\eta_T^{s,n}w)\|_{0,\Omega_2}^2 + \sum_{e \in \Gamma_h} \frac{\gamma_0}{h} \|\eta_T^{s,n}w - I_{h,h}(\eta_T^{s,n}w)\|_e^2 \\
&\quad + \sum_{e \in \Gamma_h} \frac{\gamma_0}{h} \|\eta_T^{s,n}w\|_e^2 := \mathbf{R}_1 + \mathbf{R}_2 + \mathbf{R}_3.
\end{aligned}$$

Using the fact that $\mathcal{C}_{h,H}w=0$, from (4.3) and (4.10), we have

$$\begin{aligned}
\mathbf{R}_1 &\lesssim \sum_{T \in \mathcal{T}_n \setminus \mathcal{T}_s} \|(w - \mathcal{C}_{h,H}w)\nabla\eta_T^{s,n}\|_{0,T}^2 + \|A^{\frac{1}{2}}\nabla w\|_{0,\mathcal{T}_n}^2 \\
&\lesssim \|H\nabla\eta_T^{s,n}\|_{L^\infty(\Omega)}^2 \|\nabla w\|_{0,\mathcal{T}_{n+1} \setminus \mathcal{T}_{s-1}}^2 + \|A^{\frac{1}{2}}\nabla w\|_{0,\mathcal{T}_n}^2 \\
&\lesssim \|A^{\frac{1}{2}}\nabla w\|_{0,\mathcal{T}_{n+1}}^2.
\end{aligned}$$

Further, from Lemma 4.1, it follows that

$$\begin{aligned} \mathbf{R}_2 &\lesssim \sum_{T \in \mathcal{M}_{h,\Omega_2}} \frac{\gamma_0}{h} \left(h^{-1} \|\eta_T^{s,n} w - I_{h,h}(\eta_T^{s,n} w)\|_{0,T}^2 \right. \\ &\quad \left. + \|\eta_T^{s,n} w - I_{h,h}(\eta_T^{s,n} w)\|_{0,T} \|\nabla(\eta_T^{s,n} w - I_{h,h}(\eta_T^{s,n} w))\|_{0,T} \right) \\ &\lesssim \|A^{\frac{1}{2}} \nabla(\eta_T^{s,n} w)\|_{0,\Omega_2}^2 = \mathbf{R}_1. \end{aligned}$$

For \mathbf{R}_3 , it is easy to see

$$\mathbf{R}_3 \lesssim \sum_{e \in \Gamma_h, e \subset T_n} \frac{\gamma_0}{h} \|w\|_e^2.$$

Combining the above estimates of $\mathbf{R}_1, \mathbf{R}_2$ and \mathbf{R}_3 , we have

$$\|I_{h,h}(\eta_T^{s,n} w)\|_{h,h}^2 \lesssim \|w\|_{h,h,T_{n+1}}^2,$$

470 which yields (4.11) immediately.

Next, we give the proof of the (4.12). Noting that $w \in W_{0,h}$, and $\eta_T^{s,n}|_{T_s} \equiv 1$, $\eta_T^{s,n}|_{\Omega \setminus T_n} \equiv 0$, it is obvious that

$$\begin{aligned} \|\eta_T^{s,n} w - I_{h,h}(\eta_T^{s,n} w)\|_{h,h}^2 &= \|A^{\frac{1}{2}} \nabla(\eta_T^{s,n} w - I_{h,h}(\eta_T^{s,n} w))\|_{0,T_n \setminus T_s}^2 \\ &\quad + \sum_{e \in \Gamma_h} \frac{\gamma_0}{h} \|\eta_T^{s,n} w - I_{h,h}(\eta_T^{s,n} w)\|_e^2 := \mathbf{I}_1 + \mathbf{I}_2. \end{aligned}$$

Similar to the estimate of \mathbf{R}_2 , from Lemma 4.1, it follows that

$$\mathbf{I}_2 \lesssim \mathbf{I}_1.$$

Further, by a similar argument to (B.1) and using (4.3) and (4.10), we have

$$\begin{aligned} \mathbf{I}_1 &\lesssim \|A^{\frac{1}{2}} \nabla(\eta_T^{s,n} w)\|_{0,T_n \setminus T_s}^2 \\ &\lesssim \sum_{T \in T_n \setminus T_s} \|(w - \mathcal{C}_{h,H} w) \nabla \eta_T^{s,n}\|_{0,T}^2 + \|A^{\frac{1}{2}} \nabla w\|_{0,T_n \setminus T_s}^2 \\ &\lesssim \|H \nabla \eta_T^{s,n}\|_{L^\infty(\Omega)}^2 \|\nabla w\|_{0,T_{n+1} \setminus T_{s-1}}^2 + \|A^{\frac{1}{2}} \nabla w\|_{0,T_n \setminus T_s}^2 \\ &\lesssim \|A^{\frac{1}{2}} \nabla w\|_{0,T_{n+1} \setminus T_{s-1}}^2, \end{aligned}$$

which follows (4.12) immediately. The proof of (4.13) and (4.14) is similar to the above inequality. \square

Appendix C. Proof of Lemma 4.7

The proof is divided into four steps.

Step 1. In this step we prove the following estimate for $L \geq 5$:

$$\|q_h^T - q_h^{T,L}\|_{h,h} \lesssim \|q_h^T\|_{h,h,\Omega \setminus T_{L-5}}. \quad (\text{C.1})$$

From (3.12) and (3.14), $q_h^T \in W_{0,h}$ and $q_h^{T,L} \in W_{0,h}(T_L)$ satisfy

$$\begin{aligned} a_\Omega(q_h^T, w) &= a_{\bar{T}}(u_{h,H}, w) \quad \forall w \in W_{0,h}, \\ a_\Omega(q_h^{T,L}, w) &= a_{\bar{T}}(u_{h,H}, w) \quad \forall w \in W_{0,h}(T_L). \end{aligned}$$

Subtracting the above two equations yields

$$a_\Omega(q_h^T - q_h^{T,L}, w) = 0 \quad \forall w \in W_{0,h}(T_L). \quad (\text{C.2})$$

Denote by $e := q_h^T - q_h^{T,L}$. Using the coercivity and continuity of a_Ω , from (C.2), for any $w \in W_{0,h}(T_L)$ it follows that

$$\begin{aligned} \|e\|_{h,h}^2 &\lesssim a_\Omega(e, q_h^T - q_h^{T,L}) = a_\Omega(e, q_h^T - w) \\ &\lesssim \|e\|_{h,h} \|q_h^T - w\|_{h,h}, \end{aligned}$$

which yields

$$\|q_h^T - q_h^{T,L}\|_{h,h} \lesssim \inf_{w \in W_{0,h}(T_L)} \|q_h^T - w\|_{h,h}. \quad (\text{C.3})$$

For the element T , let $\eta_T^{L-3,L-2}$ be the cut off function defined in (4.8)–(4.10) (with $l_1 = L-3, l_2 = L-2$). Since $\eta_T^{L-3,L-2} \equiv 1$ on T_{L-3} and $\eta_T^{L-3,L-2} \equiv 0$ on $\Omega \setminus T_{L-2}$, it is easy to check that:

$$\mathcal{C}_{h,H} I_{h,h}(\eta_T^{L-3,L-2} q_h^T) = \mathcal{C}_{h,H} q_h^T = 0 \quad \text{on } T_{L-4},$$

and hence

$$\text{supp}(\mathcal{C}_{h,H} I_{h,h}(\eta_T^{L-3,L-2} q_h^T)) \subseteq T_{L-1} \setminus T_{L-4}, \quad (\text{C.4})$$

$$\text{supp}(\mathcal{C}_{h,H}^2 I_{h,h}(\eta_T^{L-3,L-2} q_h^T)) \subseteq T_L \setminus T_{L-5}. \quad (\text{C.5})$$

Using Lemma 4.5, for $\mathcal{C}_{h,H}I_{h,h}(\eta_T^{L-3,L-2}q_h^T)$, there is a $\mu \in V_{0,h}$ such that

$$\begin{aligned}\mathcal{C}_{h,H}\mu &= \mathcal{C}_{h,H}I_{h,h}(\eta_T^{L-3,L-2}q_h^T), \quad \|\mu\|_{h,h} \lesssim \|\mathcal{C}_{h,H}I_{h,h}(\eta_T^{L-3,L-2}q_h^T)\|_{h,H}, \\ &\text{and } \text{supp}(\mu) \subseteq T_L \setminus T_{L-5}.\end{aligned}$$

Further, using (C.4), Lemmas 4.3 and 4.6, we have

$$\begin{aligned}\|\mu\|_{h,h} &\lesssim \|\mathcal{C}_{h,H}I_{h,h}(\eta_T^{L-3,L-2}q_h^T)\|_{h,H,T_{L-1} \setminus T_{L-4}} \\ &\lesssim \|I_{h,h}(\eta_T^{L-3,L-2}q_h^T)\|_{h,h,T_L \setminus T_{L-5}} \\ &= \|I_{h,h}(\eta_T^{L-3,L-2}q_h^T)\|_{h,h,T_{L-2} \setminus T_{L-3}} + \|q_h^T\|_{h,h,T_{L-3} \setminus T_{L-5}} \\ &\lesssim \|q_h^T\|_{h,h,T_{L-1} \setminus T_{L-5}}.\end{aligned}\tag{C.6}$$

Hence taking $w = I_{h,h}(\eta_T^{L-3,L-2}q_h^T) - \mu \in W_{0,h}(T_L)$ in (C.3) and using (C.6) and Lemma 4.6, we have

$$\begin{aligned}\|q_h^T - q_h^{T,L}\|_{h,h} &\lesssim \|I_{h,h}(1 - \eta_T^{L-3,L-2})q_h^T\|_{h,h} + \|\mu\|_{h,h} \\ &\lesssim \|q_h^T\|_{h,h,\Omega \setminus T_{L-4}} + \|q_h^T\|_{h,h,T_{L-1} \setminus T_{L-5}},\end{aligned}$$

475 which implies that (C.1) holds.

Step 2. Suppose we can prove the following recursive inequality

$$\|q_h^T\|_{h,h,\Omega \setminus T_M} \leq \theta_0 \|q_h^T\|_{h,h,\Omega \setminus T_m} \quad \forall m = M - 5 \geq 0, \tag{C.7}$$

where $0 < \theta_0 < 1$ is a constant independent of M and q_h^T .

For $L = 5k + j$ with integers $k \geq 1$ and $0 \leq j \leq 4$, setting $\theta = \theta_0^{\frac{1}{5}}$ and using (C.7) repeatedly, we conclude that

$$\begin{aligned}\|q_h^T\|_{h,h,\Omega \setminus T_{L-5}} &\lesssim \theta_0^{k-1} \|q_h^T\|_{h,h,\Omega \setminus T_j} \lesssim \theta^{L-j-5} \|q_h^T\|_{h,h} \\ &\lesssim \theta^L \|q_h^T\|_{h,h}.\end{aligned}\tag{C.8}$$

Clearly, the above estimate also holds for $5 \leq L \leq 9$ and hence (C.8) holds for $L \geq 5$.

Step 3. In this step we prove (C.7). Let $\varepsilon = 1 - \eta_T^{m+2,M-2}$ satisfying $\varepsilon \equiv 1$ in $\Omega \setminus T_{M-2}$, $\varepsilon \equiv 0$ in T_{m+2} , and $0 < \varepsilon < 1$ otherwise. It is easy to see that

$$\begin{aligned}\|q_h^T\|_{h,h,\Omega \setminus T_M}^2 &\leq \|\varepsilon q_h^T\|_{h,h}^2 \lesssim a_\Omega(\varepsilon q_h^T, \varepsilon q_h^T) \\ &= a_\Omega(q_h^T, \varepsilon^2 q_h^T) + (A \nabla_h \varepsilon \cdot q_h^T, \nabla_h \varepsilon \cdot q_h^T).\end{aligned}\tag{C.9}$$

For the function $\mathcal{C}_{h,H}I_{h,h}(\varepsilon^2 q_h^T)$, using Lemma 4.5, there exists a $\gamma \in V_{0,h}$ such that $\mathcal{C}_{h,H}\gamma = \mathcal{C}_{h,H}I_{h,h}(\varepsilon^2 q_h^T)$, and

$$\begin{aligned} \text{supp}(\mathcal{C}_{h,H}I_{h,h}(\varepsilon^2 q_h^T)) &\subseteq T_{M-1} \setminus T_{m+1}, \\ \text{supp}(\gamma) &\subseteq \text{supp}(\mathcal{C}_{h,H}^2 I_{h,h}(\varepsilon^2 q_h^T)) \subseteq T_M \setminus T_m. \end{aligned}$$

In addition, it holds that

$$\|\gamma\|_{h,h} \lesssim \|\mathcal{C}_{h,H}I_{h,h}(\varepsilon^2 q_h^T)\|_{h,H}. \quad (\text{C.10})$$

Since $I_{h,h}(\varepsilon^2 q_h^T) - \gamma \in W_{0,h}(\Omega_2 \setminus T_m)$, from (3.12), it follows that

$$a_\Omega(q_h^T, I_{h,h}(\varepsilon^2 q_h^T) - \gamma) = a_{\bar{T}}(u_{h,H}, I_{h,h}(\varepsilon^2 q_h^T) - \gamma) = 0,$$

which combines (C.9) yields

$$\begin{aligned} \|q_h^T\|_{h,h,\Omega \setminus T_M}^2 &\lesssim a_\Omega(q_h^T, \varepsilon^2 q_h^T - I_{h,h}(\varepsilon^2 q_h^T)) + a_\Omega(q_h^T, \gamma) \\ &\quad + (A\nabla\varepsilon \cdot q_h^T, \nabla\varepsilon \cdot q_h^T) := \mathsf{T}_1 + \mathsf{T}_2 + \mathsf{T}_3. \end{aligned}$$

Using the same argument as that of (4.12), we obtain

$$\begin{aligned} \mathsf{T}_1 &\lesssim \|q_h^T\|_{h,h,T_{M-2} \setminus T_{m+2}} \|\varepsilon^2 q_h^T - I_{h,h}(\varepsilon^2 q_h^T)\|_{h,h,T_{M-2} \setminus T_{m+2}} \\ &\lesssim \|q_h^T\|_{h,h,T_{M-1} \setminus T_{m+1}}^2. \end{aligned}$$

Further, for T_2 , using the same argument as that of (4.11), from (C.10), we have

$$\begin{aligned} \mathsf{T}_2 &\lesssim \|q_h^T\|_{h,h,T_M \setminus T_m} \|\gamma\|_{h,h} \\ &\lesssim \|q_h^T\|_{h,h,T_M \setminus T_m} \|\mathcal{C}_{h,H}I_{h,h}(\varepsilon^2 q_h^T)\|_{h,H,T_{M-1} \setminus T_{m+1}} \\ &\lesssim \|q_h^T\|_{h,h,T_M \setminus T_m} \|I_{h,h}(\varepsilon^2 q_h^T)\|_{h,h,T_M \setminus T_m} \\ &= \|q_h^T\|_{h,h,T_M \setminus T_m} (\|q_h^T\|_{h,h,T_M \setminus T_{M-2}} + \|I_{h,h}(\varepsilon^2 q_h^T)\|_{h,h,T_{M-2} \setminus T_{m+2}}) \\ &\lesssim \|q_h^T\|_{h,h,T_M \setminus T_m}^2. \end{aligned}$$

To estimate T_3 , by use of the assumption (4.8)–(4.10) and (4.3), it follows that

$$\begin{aligned} T_3 &= \|A^{\frac{1}{2}} \nabla \varepsilon \cdot q_h^T\|_{0,\Omega}^2 = \sum_{T \in \mathcal{M}_{H,\Omega_2}} \|A^{\frac{1}{2}} \nabla \varepsilon \cdot q_h^T\|_{0,T}^2 \\ &\lesssim \sum_{T \in T_{M-2} \setminus T_{m+2}} \|\nabla \varepsilon\|_{L^\infty(\Omega)}^2 \|q_h^T - \mathcal{C}_H q_h^T\|_{0,T}^2 \\ &\lesssim \|q_h^T\|_{h,h,T_{M-1} \setminus T_{m+1}}^2. \end{aligned}$$

Thus, by using the above estimates of T_1 , T_2 , and T_3 , we have, for some positive constant C_0 ,

$$\|q_h^T\|_{h,h,\Omega \setminus T_M}^2 \leq C_0 \|q_h^T\|_{h,h,T_M \setminus T_m}^2 = C_0 \|q_h^T\|_{h,h,\Omega \setminus T_m}^2 - C_0 \|q_h^T\|_{h,h,\Omega \setminus T_M}^2,$$

which implies that (C.7) holds with $\theta_0 := \left(\frac{C_0}{C_0+1}\right)^{\frac{1}{2}}$.

Step 4. Next, we estimate $\|q_h^T\|_{h,h}^2$ in (C.8).

$$\|q_h^T\|_{h,h}^2 \lesssim a_\Omega(q_h^T, q_h^T) = a_{\tilde{T}}(u_{h,H}, q_h^T) \lesssim \|u_{h,H}\|_{h,h,\tilde{T}} \|q_h^T\|_{h,h},$$

480 where \tilde{T} is defined in Section 3.4, which together with (C.1) and (C.8) completes
the proof of the lemma. \square

References

References

- [1] I. Babuška, G. Caloz, J. Osborn, Special finite element methods for a class
485 of second order elliptic problems with rough coefficients, SIAM J. Numer.
Anal. 31 (1994) 945–981.
- [2] I. Babuška, U. Banerjee, J. E. Osborn, Survey of meshless and generalized
finite element methods: a unified approach, Acta Numer. 12 (2003) 1–125.
- [3] T. Strouboulis, I. Babuška, K. Copps, The design and analysis of the gener-
490 alized finite element method, Comput. Methods Appl. Mech. Engrg. 181 (1-
3) (2000) 43–69.

- [4] T. Y. Hou, X. H. Wu, A multiscale finite element method for elliptic problems in composite materials and porous media, *J. Comput. Phys.* 134 (1997) 169–189.
- 495 [5] Y. Efendiev, T. Y. Hou, X. H. Wu, Convergence of a nonconforming multiscale finite element method, *SIAM J. Numer. Anal.* 37 (2000) 888–910.
- [6] Z. Chen, T. Y. Hou, A mixed multiscale finite method for elliptic problems with oscillating coefficients, *Math. Comp.* 72 (2002) 541–576.
- 500 [7] T. Hughes, Multiscale phenomena: Green’s functions, the dirichlet to neumann formulation, subgrid scale models, bubbles and the origin of stabilized methods, *Comput. Meth. Appl. Mech. Eng.* 127 (1995) 387–401.
- [8] T. J. R. Hughes, G. R. Feijóo, L. Mazzei, J.-B. Quincy, The variational multiscale method—a paradigm for computational mechanics, *Comput. Methods Appl. Mech. Engrg.* 166 (1-2) (1998) 3–24.
- 505 [9] F. Brezzi, L. P. Franca, T. J. R. Hughes, A. Russo, $b = \int g$, *Comput. Methods Appl. Mech. Engrg.* 145 (1997) 329–339.
- [10] J. Fish, Z. Yuan, Multiscale enrichment based on partition of unity, *Inter. J. Numer. Meth. Eng.* 62 (2005) 1341–1359.
- [11] W. E, B. Engquist, The heterogeneous multiscale methods, *Commun. Math. Sci.* 1 (2003) 87–132.
- 510 [12] W. E, P. Ming, P. Zhang, Analysis of the heterogeneous multiscale method for elliptic homogenization problems, *J. Am. Math. Soc.* 18 (2005) 121–156.
- [13] A. Abdulle, W. E, B. Engquist, E. Vanden-Eijnden, The heterogeneous multiscale method, *Acta Numer.* 21 (2012) 1–87.
- 515 [14] P. Jenny, S. Lee, H. Tchelepi, Multi-scale finite-volume method for elliptic problems in subsurface flow simulation, *J. Comput. Phys.* 187 (1) (2003) 47–67.

- [15] J. Fish, V. Belsky, Multigrid method for periodic heterogeneous media. I. Convergence studies for one-dimensional case, *Comput. Methods Appl. Mech. Engrg.* 126 (1-2) (1995) 1–16.
- [16] H. Owhadi, Multigrid with rough coefficients and multiresolution operator decomposition from hierarchical information games, *SIAM Rev.* 59 (1) (2017) 99–149.
- [17] M. F. Wheeler, Mortar upscaling for multiphase flow in porous media, *Computational Geosciences* 6 (1) (2002) 73–100.
- [18] T. Arbogast, G. Pencheva, M. F. Wheeler, I. Yotov, A multiscale mortar mixed finite element method, *Multiscale Model. Simul.* 6 (1) (2007) 319–346.
- [19] A. Målqvist, D. Peterseim, Localization of elliptic multiscale problems, *Math. Comp.* 83 (290) (2014) 2583–2603.
- [20] P. Henning, D. Peterseim, Oversampling for the multiscale finite element method, *Multiscale Model. Simul.* 11 (4) (2013) 1149–1175.
- [21] P. Henning, A. Målqvist, Localized orthogonal decomposition techniques for boundary value problems, *SIAM J. Sci. Comput.* 36 (4) (2014) A1609–A1634.
- [22] A. J. Roberts, I. G. Kevrekidis, General tooth boundary conditions for equation free modeling, *SIAM J. Sci. Comput.* 29 (4) (2007) 1495–1510.
- [23] A. Papavasiliou, I. G. Kevrekidis, Variance reduction for the equation-free simulation of multiscale stochastic systems, *Multiscale Model. Simul.* 6 (1) (2007) 70–89.
- [24] Y. Efendiev, J. Galvis, T. Y. Hou, Generalized multiscale finite element methods (GMsFEM), *J. Comput. Phys.* 251 (2013) 116–135.

- [25] E. T. Chung, Y. Efendiev, T. Y. Hou, Adaptive multiscale model reduction with generalized multiscale finite element methods, *J. Comput. Phys.* 320 (2016) 69–95.
- 545
- [26] I. Babuška, R. Lipton, P. Sinz, M. Stuebner, Multiscale-spectral GFEM and optimal oversampling, *Comput. Methods Appl. Mech. Engrg.* 364 (2020) 112960, 28.
- [27] I. Babuska, R. Lipton, Optimal local approximation spaces for generalized finite element methods with application to multiscale problems, *Multiscale Model. Simul.* 9 (1) (2011) 373–406.
- 550
- [28] E. T. Chung, Y. Efendiev, W. T. Leung, Constraint energy minimizing generalized multiscale finite element method, *Comput. Methods Appl. Mech. Engrg.* 339 (2018) 298–319.
- [29] E. T. Chung, Y. Efendiev, W. T. Leung, Generalized multiscale finite element methods with energy minimizing oversampling, *Internat. J. Numer. Methods Engrg.* 117 (3) (2019) 316–343.
- 555
- [30] M. Li, E. T. Chung, L. Jiang, A constraint energy minimizing generalized multiscale finite element method for parabolic equations, *Multiscale Model. Simul.* 17 (3) (2019) 996–1018.
- 560
- [31] H. Owhadi, L. Zhang, Metric-based upscaling, *Comm. Pure Appl. Math.* 60 (5) (2007) 675–723.
- [32] H. Owhadi, L. Zhang, Localized bases for finite-dimensional homogenization approximations with nonseparated scales and high contrast, *Multiscale Model. Simul.* 9 (2011) 1373–1398.
- 565
- [33] L. Durlafsky, Numerical calculation of equivalent grid block permeability tensors for heterogeneous porous media, *Water Resources Research* 27 (1991) 699–708.

- [34] T. Arbogast, Numerical subgrid upscaling of two-phase flow in porous media, in: Z. Chen, R. E. Ewing, Z. C. Shi (Eds.), Numerical Treatment of Multiphase Flows in Porous Media, Vol. 552 of Lect. Notes Phys., Springer-Verlag, New York, 2000, pp. 35–49.
- [35] X. H. Wu, Y. Efendiev, T. Y. Hou, Analysis of upscaling absolute permeability, Discrete and Continuous Dynamical Systems-series B (2002) 185–204.
- [36] Y. Efendiev, J. Galvis, X. H. Wu, Multiscale finite element methods for high-contrast problems using local spectral basis functions, J. Comput. Phys. 230 (4) (2011) 937–955.
- [37] J. Galvis, Y. Efendiev, Domain decomposition preconditioners for multiscale flows in high-contrast media, Multiscale Model. Simul. 8 (2010) 1461–1483.
- [38] J. Galvis, Y. Efendiev, Domain decomposition preconditioners for multiscale flows in high-contrast media: Reduced dimension coarse spaces, Multiscale Model. Simul. 8 (2010) 1621–1644.
- [39] Z. Chen, X. Y. Yue, Numerical homogenization of well singularities in the flow transport through heterogeneous porous media, Multiscale Model. Simul. 1 (2003) 260–303.
- [40] E. T. Chung, Y. Efendiev, G. Li, An adaptive GMsFEM for high-contrast flow problems, J. Comput. Phys. 273 (2014) 54–73.
- [41] E. T. Chung, Y. Efendiev, W. T. Leung, An adaptive generalized multiscale discontinuous Galerkin method for high-contrast flow problems, Multiscale Model. Simul. 16 (3) (2018) 1227–1257.
- [42] C. C. Chu, I. G. Graham, T. Y. Hou, A new multiscale finite element method for high-contrast elliptic interface problems, Math. Comp. 79 (272) (2010) 1915–1955.

- [43] D. Elfverson, M. G. Larson, A. Målqvist, Multiscale methods for problems with complex geometry, *Comput. Methods Appl. Mech. Engrg.* 321 (2017) 103–123.
- [44] F. Hellman, A. Målqvist, Contrast independent localization of multiscale problems, *Multiscale Model. Simul.* 15 (4) (2017) 1325–1355.
- [45] W. Deng, H. Wu, A combined finite element and multiscale finite element method for the multiscale elliptic problems, *Multiscale Model. Simul.* 12 (4) (2014) 1424–1457.
- [46] F. Song, W. Deng, H. Wu, A combined finite element and oversampling multiscale Petrov-Galerkin method for the multiscale elliptic problems with singularities, *J. Comput. Phys.* 305 (2016) 722–743.
- [47] D. Elfverson, E. H. Georgoulis, A. Målqvist, D. Peterseim, Convergence of a discontinuous Galerkin multiscale method, *SIAM J. Numer. Anal.* 51 (6) (2013) 3351–3372.
- [48] D. Elfverson, V. Ginting, P. Henning, On multiscale methods in petrov-galerkin formulation, *Numerische Mathematik* (2015) 1–40.
- [49] P. Henning, P. Morgenstern, D. Peterseim, Multiscale partition of unity, in: *Meshfree methods for partial differential equations VII*, Vol. 100 of *Lect. Notes Comput. Sci. Eng.*, Springer, Cham, 2015, pp. 185–204.
- [50] P. Henning, A. Målqvist, D. Peterseim, A localized orthogonal decomposition method for semi-linear elliptic problems, *ESAIM Math. Model. Numer. Anal.* 48 (5) (2014) 1331–1349.
- [51] A. Målqvist, D. Peterseim, Computation of eigenvalues by numerical up-scaling, *Numer. Math.* 130 (2) (2014) 337–361.
- [52] P. Henning, A. Målqvist, D. Peterseim, Two-level discretization techniques for ground state computations of Bose-Einstein condensates, *SIAM J. Numer. Anal.* 52 (4) (2014) 1525–1550.

- [53] C. Engwer, P. Henning, A. Målqvist, D. Peterseim, Efficient implementation of the localized orthogonal decomposition method, *Comput. Methods Appl. Mech. Engrg.* 350 (2019) 123–153.
- [54] D. Peterseim, Variational multiscale stabilization and the exponential decay of fine-scale correctors, in: *Building bridges: connections and challenges in modern approaches to numerical partial differential equations*, Vol. 114 of *Lect. Notes Comput. Sci. Eng.*, Springer, [Cham], 2016, pp. 341–367.
- [55] H. Cao, H. Wu, IPCDGM and multiscale IPDPGM for the Helmholtz problem with large wave number, *J. Comp. Appl. Math.* 369 (2020) 112590.
- [56] S. C. Brenner, L. R. Scott, *The mathematical theory of finite element methods*, Springer-Verlag, New York, 2002.
- [57] D. Arnold, An interior penalty finite element method with discontinuous elements, *SIAM J. Numer. Anal.* 19 (1982) 742–760.
- [58] C. Carstensen, Quasi-interpolation and a posteriori error analysis in finite element methods, *M2AN Math. Model. Numer. Anal.* 33 (1999) 1187–1202.
- [59] C. Carstensen, R. Verfürth, Edge residuals dominate a posteriori error estimates for low order finite element methods, *SIAM J. Numer. Anal.* 36 (1999) 1571–1587.
- [60] P. Ciarlet, *The Finite Element Method for Elliptic Problems*, Amsterdam, North Holland, 1978.
- [61] L. Durlofsky, Numerical calculation of equivalent grid block permeability tensors for heterogeneous porous media, *Water Resources Res.* 27 (1991) 699–708.
- [62] D. W. Peaceman, Interpretation of well-block pressures in numerical reservoir simulations with non-square grid blocks and anisotropic permeability, *Soc. Pet. Eng. J.* 23 (1983) 531–543.